

Lagutin A.A., Uchaikin V.V.

Adjoint Cascade Theory in Astroparticle Physics

Adjoint approach to the astroparticle physic problems is presented. Several problems are considered to demonstrate the usefulness and practical applications of adjoint formalism.

Introduction

The interactions of high energy cosmic rays are investigated usually from the cascades they produce in the atmosphere, rock or detector. A theory of cascade process is necessary to analyse and interpret the observations.

In the conventional cascade theory [1–4] the mathematical description on the cascade process is based on the Boltzmann kinetic equation for particle flux density f_α . The time-independent equation has the well-known form

$$\Omega \nabla f_\alpha + \sigma_\alpha f_\alpha - \sum_\beta \int d\Omega' \int dE' w_{\beta\alpha}(\Omega' \rightarrow \Omega, E' \rightarrow E) f_\beta(\mathbf{r}, \Omega', E') = s_\alpha, \quad (1)$$

where index α means a kind of particle, $w_{\alpha\beta}(\Omega \rightarrow \Omega', E \rightarrow E')$ is inclusive spectre of particle β in α -nuclear interaction,

$$\int d\Omega' \int dE' w_{\alpha\beta}(\Omega \rightarrow \Omega', E \rightarrow E') = \sigma_\alpha \bar{n}_{\alpha\beta},$$

s is the source and other notations are traditional. In operator form these basic equations can be written as

$$Lf = s, \quad (2)$$

where L is kinetic operator. However, very important point is that the particle distribution f_α itself can be never observed; only the effects of the distribution are observable. The observable may be the collision rate in a finite volume, track length of the shower electrons, number of Čerenkov quanta or any number of other quantities.

In transport theory the radiation field information obtained in experiments or calculations is formalized by introduction of detector conception and detector response function d_α [5], which equals to the contribution of the unit way of the α -kind particle at point (\mathbf{r}, Ω, E) of the phase space to detector reading (or response) \bar{Q} :

$$\bar{Q} = \sum_\alpha \iiint d_\alpha(\mathbf{r}, \Omega, E) f_\alpha(\mathbf{r}, \Omega, E) d\mathbf{r} d\Omega dE$$

or

$$\bar{Q} = (d, f). \quad (3)$$

Here, for convenience sake, integrals over all phase space $x = (\mathbf{r}, \Omega, E)$ and sum over α are denoted by parentheses as an inner product of two functions.

Thus, to find any detector reading of interest in the conventional cascade theory, it is necessary to solve basic equations (1) for f_α and then calculate \bar{Q} using equation (3).

Strictly speaking, the analysis of experimental data in cosmic rays is performed to solve the inverse problems, that is, it needs to determine the primary spectrum, feature of the particle interactions in high energy region (cross section, multiplicity, etc.) or other characteristics of cosmic rays using observable values (3). For example, in paper [6] the reconstruction of average cascade curve of EAS electrons $N(z, E)$ on the lateral distribution of their atmospheric Čerenkov light flux density $q(z^*, r, E)$,

$$q(z^*, r, E) = \int_0^{z^*} dz G(r, z, \dots) N(z, E),$$

measured at observation level z^* by a method of inverse problem was attempted.

However, it is clear that before trying to solve an inverse problem it is necessary to investigate the sensitivity of used observable values with respect to value of interest. Fluctuations in the cascade characteristics also play an essential role in the analysis of the shower phenomena. Importance of the fluctuations and sensitivity analysis has already been pointed out in the original works [7,8], but in view of mathematical difficulties these problems were attacked mostly by Monte Carlo method.

With the improvement of the experimental techniques, the accumulation of the data and, hence, the increasing requirements on accuracy of the cascade calculations it seems actual to develop adequate mathematical methods which enable to

solve the problems necessary for the design studies of new experiments, increasing sensitivity of experimental methods and interpreting observational data on the up-to-date level.

An alternative approach to conventional cascade theory is Monte Carlo method. As is well known, the Monte Carlo simulations of particle transport in matter allows an almost exact treatment of all physical processes. However, despite this potential the method suffers from the severe limitation that sensitivity studies are either very expensive or even impossible, if the expected difference of the sampled responses are comparable in size to their errors. For this reason, Monte Carlo calculations can not be considered as tools for sensitivity studies, optimization and solving inverse problems.

The mathematical formulation of the cascade problems in cosmic rays mentioned above based on the adjoint approach [5,9–11] in our opinion is more closely related to the actual experiments. This approach leads to similar expressions for the adjoint equations, adjoint moment equations and the sensitivity function equations. That is, it allows to calculate in unified manner mean values, fluctuations and sensitivity functions of quantities of interest. Since most problems of interest are not amenable to analytical solutions, the same numerical method can be used to solve the equations listed above. In this case the results do not suffer from difficulties inherent in Monte Carlo simulations, namely the statistical fluctuations of results and linear increase of computing time with increasing initial energy.

The main goal of this paper is to discuss some recent trends and methods in describing cascade processes in cosmic rays via the adjoint equations. We will attempt to present sufficient material to allow the reader to see some of the advantages of the adjoint approach, but we shall not undertake to give a complete review. For the discussion of various related subjects, the reader is referred to the works [5,9–13].

The organization of this paper is as follows. In Sec. 1 we introduce an adjoint function and write adjoint equation. Then the duality principle is discussed. In Sec. 2 the adjoint equations for several cascade problems under different approximations are presented. As example, we derive one-dimensional and three-dimensional adjoint equations of electromagnetic cascade, one-dimensional adjoint equation of extensive air shower (EAS). We also write adjoint equation governing the muon transport in rock. In Sec. 3 the duality principle in the fluctuation problems is discussed. The adjoint equations in fluctuation problems are presented in

Sec. 4. In Sec. 5 a short review of a numerical method for solving adjoint equation of cascade theory is presented. To demonstrate the usefulness of adjoint formalism in ‘classical’ cascade problems, in Sec. 6,7 our results of cascade characteristic calculations are discussed. In Sec. 8 we consider the mathematical formulation of the sensitivity theory based on the use of adjoint functions. Then, in Sec. 9–11 the sensitivity theory in the problems highest energy EAS simulation, sensitivity of cosmic ray muon component to electric field in the atmosphere and the AGN’s gamma-ray spectra and their variations in the cascade model are considered to illustrate practical applications of the sensitivity formalism.

1. Duality principle. Adjoint function

As known, the evolution of a particle cascade can be derived in two equivalent ways [13], i.e. via basic cascade equation $Lf = s$, mentioned above, and adjoint equation

$$L^+ f^+ = d. \quad (4)$$

In the equation (4) f^+ is adjoint function, L^+ is adjoint cascade operator which obeys the following equality

$$\int f^+ Lf dx = \int f L^+ f^+ dx$$

or

$$(f^+, Lf) = (f, L^+ f^+).$$

The adjoint equation can be derived by defining adjoint of the operator L . Then, in explicit mathematical form this equation can be written as

$$-\Omega \nabla f_\alpha^+ + \sigma_\alpha f_\alpha^+ - \sum_\beta \int d\Omega' \int dE' w_{\alpha\beta}(\Omega \rightarrow \Omega', E \rightarrow E') f_\beta^+(\mathbf{r}, \Omega', E') = d_\alpha. \quad (5)$$

The main difference between the basic and adjoint equations is that in basic equation (1) the final phase coordinates are the operational variables and the initial coordinates are parameters, whereas in adjoint equation (5) it is the other way round.

The relationship between the detector reading \bar{Q} and the solution of the adjoint equation f_α^+ is given by the expression

$$\bar{Q} = (f^+, s). \quad (6)$$

The equations (3), (6) reflect the well-known duality principle [13]. The equivalence of these results is easily demonstrated by multiplying (4) by f and (2) by f^+ , integrating over all phase space and subtracting the two resulting equations.

From formula (6) it is possible to understand the sense of adjoint function. If the source s is a multi-dimensional delta-function $\delta(x - x_0)$, then

$$\bar{Q} = f^+(x_0).$$

This result demonstrates that the adjoint function $f^+(x_0)$ represents the contribution of cascade generated by one particle at point x_0 in phase space to result \bar{Q} . Because of this property of the adjoint function, it can be physically interpreted as an importance function or importance [12,13].

It is interesting to note that the procedures for solving the adjoint equations are completely the opposite to those that would be used in the conventional theory. The adjoint problem solution is started at a final ‘time’ with the detector function d as the source, and the equations are solved moving backward in ‘time’. This reversal of procedures is typical of all adjoint problems and is consistent with the physical interpretation of the adjoint solutions as importance functions for a response \bar{Q} .

Particular attention must be focused on the symmetry of the source s and detector function d . If the symmetry of the system ‘medium+detector’ is higher one of the system ‘medium+source’, the adjoint equations contain less number of independent variables than the basic equations and hence are simple to be solved. Such situation is realised in the radial distribution problem [14] (see, also, Sec. 2). In this problem the source is mono-directional (i.e. cylindrical symmetry of the source), but the detector is isotropic (spherical symmetry).

For high energy particles the scattering is very anisotropic and peaked in the forward direction. By neglecting the deflection due to the scattering of a particle the adjoint equation (5) is reduced to

$$-\frac{\partial f_\alpha^+}{\partial z} + \sigma_\alpha f_\alpha^+ - \sum_\beta \int dE' w_{\alpha\beta}(E \rightarrow E') f_\beta^+(z, E') = d_\alpha. \quad (7)$$

Note, that in this section a usual route for derivation of the adjoint equation was presented. To discuss a straightforward way for their derivation based on the importance conservation law the reader is referred to the works [9–11].

2. Adjoint equations

To make the results of the derivations in preceding section more understandable, the adjoint equations for several cascade problems under different approximations are presented.

One-dimensional adjoint equations of electromagnetic cascade

The one-dimensional adjoint equations of electromagnetic cascade are:

$$-\frac{\partial}{\partial z} N_e(z, E) + \sigma_e(E) N_e(z, E) - \int_{E_{th}}^E dE' w_{ee}(E \rightarrow E') N_e(z, E') - \int_{E_{th}}^E dE' w_{e\gamma}(E \rightarrow E') N_\gamma(z, E') = d_e, \quad (8)$$

$$-\frac{\partial}{\partial t} N_\gamma(z, E) + \sigma_\gamma(E) N_\gamma(z, E) - \int_{E_{th}}^E dE' w_{\gamma e}(E \rightarrow E') N_e(z, E') - \int_{E_{th}}^E dE' w_{\gamma\gamma}(E \rightarrow E') N_\gamma(z, E') = d_\gamma. \quad (9)$$

Three-dimensional adjoint equations of electromagnetic cascade

Consider a point detector measuring the integrated over angles flux of electrons with the energies higher than threshold E_{th} that is placed in infinite homogeneous medium. The primary particle with the energy E generating the shower is at the distance t of it. According to the evident symmetry the readings of such a detector, except the energies E and E_{th} will depend on t and the angle θ between the primary particle movement direction and the direction towards the detector. Let us mark the detector readings by $N_e(t, \theta, E)$ and $N_\gamma(t, \theta, E)$ in the case of a primary electron and photon accordingly. Since, the high energy particle penetration is dominated by small-angle scattering, the small angle approximation can be used. In this approximation the functions N_e, N_γ satisfy the ad-

joint equations which have the form:

$$\begin{aligned} \left[\frac{\partial}{\partial t} - \frac{\theta}{t} \frac{\partial}{\partial \theta} + \sigma_e(E) \right] N_e(t, \theta, E) = \\ = \int_{E_{th}}^E dE' w_{ee}(E \rightarrow E') N_e(t, \theta, E') + \\ + \int_{E_{th}}^E dE' w_{e\gamma}(E \rightarrow E') N_\gamma(t, \theta, E') - \\ - \int_0^{2\pi} d\phi \int_0^\infty w_s(E, \Theta) [N_e(t, \theta, E) - \\ - N_e(t, \theta', E)] \theta' d\theta', \quad (10) \end{aligned}$$

$$\begin{aligned} \left[\frac{\partial}{\partial t} - \frac{\theta}{t} \frac{\partial}{\partial \theta} + \sigma_\gamma(E) \right] N_\gamma(t, \theta, E) = \\ = \int_{E_{th}}^E dE' w_{\gamma e}(E \rightarrow E') N_e(t, \theta, E') + \\ + \int_{E_{th}}^E dE' w_{\gamma\gamma}(E \rightarrow E') N_\gamma(t, \theta, E'), \quad (11) \end{aligned}$$

where $w_s(E, \Theta)$ is a differential cross-section of Coulomb scattering to the angle $\Theta = \sqrt{\theta^2 + \theta'^2 - 2\theta\theta' \cos \phi}$, $t = z^* - z$ is the distance between a primary particle and plane, where boundary conditions are defined. Boundary conditions for N_e and N_γ have the form:

$$\begin{aligned} \lim_{t \rightarrow 0} 2\pi t^2 N_e(t, \theta, E) = \begin{cases} \delta(\theta)/\theta, & E \geq E_{th}, \\ 0, & E < E_{th}, \end{cases} \\ \lim_{t \rightarrow 0} 2\pi t^2 N_\gamma(t, \theta, E) = 0. \end{aligned}$$

Note that in the small angle approximation the variable t can be interpreted as the distance from the primary particle along its movement direction to the observation plane which is perpendicular to this direction. The radius r of the observation point in this plane is expressed through θ by the relation $r = \theta t$.

One-dimensional adjoint equations of EAS: muon component

The adjoint equations describing the muon component of EAS in the model when three kinds of cascade particles $\alpha = N, \pi, \mu$ are taken into ac-

count have the form

$$\begin{aligned} - \frac{\partial f_N^+}{\partial z} + \sigma_N f_N^+ - \int dE' w_{NN}(E \rightarrow E') f_N^+(z, E') - \\ - \int dE' w_{N\pi}(E \rightarrow E') f_\pi^+(z, E') = 0, \quad (12) \end{aligned}$$

$$\begin{aligned} - \frac{\partial f_\pi^+}{\partial z} + (\sigma_\pi + \sigma_\pi^r) f_\pi^+ - \\ - \int dE' w_{\pi\pi}(E \rightarrow E') f_\pi^+(z, E') - \\ - \sigma_\pi^r \int dE' w_{\pi\mu}(E \rightarrow E') f_\mu^+(z, E') = 0, \quad (13) \end{aligned}$$

$$\begin{aligned} - \frac{\partial f_\mu^+}{\partial z} + \sigma_\mu^r f_\mu^+ + \beta_\mu \frac{\partial f_\mu^+}{\partial E} = \\ = \delta(z - z^*) \varepsilon(E - E_{th}), \quad (14) \end{aligned}$$

where σ_π^r is a cross section for decay $\pi \rightarrow \mu$, $\varepsilon(x)$ is Heaviside unit step function.

Adjoint equation for muon component in rock

Adjoint equation governing the muon transport in rock have the form

$$\begin{aligned} - \frac{\partial P(z, E)}{\partial z} + \sigma_\mu P(z, E) - \\ - \sum_{\beta=i,p,b,n} \int dE' w_{\mu\beta}(E \rightarrow E') P(z, E - E') = d_\mu. \quad (15) \end{aligned}$$

Here $w_{\mu\beta}(E \rightarrow E')$ is a differential cross section for muon interaction of type β : knock-on electron production (i), pair production (p), bremsstrahlung (b) and photonuclear interaction (n),

$$\sigma_\mu(E) = \sum_{\beta=i,p,b,n} \int dE' w_{\mu\beta}(E \rightarrow E').$$

Note, that if $d_\mu = \delta(z - z^*) \varepsilon(E - E_{th})$ then the adjoint function $P(z, E)$ is known as survival probability.

3. Duality principle in the fluctuation problems

If we want to know a value of fluctuations of detector reading the equation (1) or (5) is deficient for that. The simplest characteristic of the fluctuation is the variance:

$$\mathbf{DQ} = \overline{Q^2} - \bar{Q}^2.$$

The second statistical moment $\overline{Q^2}$ has two equivalent representations too:

$$\overline{Q^2} = \int d^{(2)}(x)f(x)dx + \int \int d(x_1)d(x_2)f_2(x_1, x_2)dx_1dx_2, \quad (16)$$

$$\overline{Q^2} = \int f^{+(2)}(x)s(x)dx + \int \int f^+(x_1)f^+(x_2)s_2(x_1, x_2)dx_1dx_2. \quad (17)$$

The functions f_2 and s_2 are so-called product density functions [15] or, more strictly, density of the second factorial moment [9]. The functions $d^{(2)}$ and s_2 are responsible for the statistical fluctuations in the detector and in the source respectively. The function $f^{+(2)}(x)$ is the mean square of detector reading made by a cascade from a single primary particle starting in the point x :

$$f^{+(2)} = \overline{q^2}(x).$$

If the first (basic) way is chosen we have to use the formula (16) and the following equation for f_2 :

$$\begin{aligned} L(x_1)f_2(x_1, x_2) + L(x_2)f_2(x_1, x_2) = \\ = s_2(x_1, x_2) + h_2(x_1, x_2), \end{aligned} \quad (18)$$

where $h_2(x_1, x_2)$ is the function which includes an information about $f(x)$.

If the second (adjoint) way is taken we use the formula (17) and the following equation for $f^{+(2)}(x)$:

$$L(x_1)f^{+(2)}(x) = d^{(2)}(x) + g^{(2)}(x), \quad (19)$$

where $g^{(2)}(x)$ contains an information about $f^+(x)$.

Both ways are equivalent although the equations (18) and (19) have different forms. The difference may be easily explained if we take into account that the mathematical process of conjugation contains the change of the time sign. Obviously cascade processes are no time symmetrical, because particles are able to be born together but die one by one only.

The adjoint way allows us to obtain an equation for the probability distribution density $\psi(q|x)$ which is connected with the distribution of detector reading $\psi(q)$ by the following relationship:

$$\psi(q) = \int \psi(q|x)s(x)dx.$$

It is obvious that

$$\overline{Q^n} = \int Q^n \psi(Q)dQ, \quad \overline{q^n}(x) = \int q^n \psi(q|x)dx.$$

The basic equations of the second order (18) appeared in the works of Bhabha and Ramakrishnan [16,17] in 1950. At first the adjoint approach to cascade problem was used by Janossy in the same year [18]. He obtained adjoint equation for generating function of number of particles in fixed depth of a matter (G - equation), then he derived equations for the first and the second moments like (4),(19) and resolved them in A-approximation of electromagnetic cascade (EMC) theory. The detailed review of the early works of this trend was given in the books [19,20]. Lately Gerasimova [21] and Gedalin [22] obtained the solution of this problem in B-approximation of the cascade theory using the saddle point technique. But the more latest experimental investigations [23–25] showed that the analytical methods are rougher in fluctuation problems than in calculations of mean values. A rough description of elementary processes cause the difference between analytical and experimental results, too.

There was a suitable example of such a situation. We mean the works [26] in which a number of arising particles was investigated. The authors obtained nonzero limit of relatively fluctuations of the number by the incident energy $E \rightarrow \infty$ though experiments gave $E^{-1/2}$. They used only the main asymptotical term of the mean number in calculating of fluctuations. We have shown that using of the exact mean number leads to correct asymptotic behaviour of fluctuations [27].

The fluctuation problem became more important as cosmic ray and accelerator experimental research developed. The stating of the problem changed from academician one to real experimental conditions. That what stimulated the development of calculation technique, especially numerical one.

Monte Carlo technique has been used in fluctuation problems since the fifties. This technique does not require simple analytical expressions for elementary processes but its results have statistical errors which decrease too slowly with calculation time. For this reason the Monte Carlo method (in its pure form) is not useful for investigation of the fluctuations of very high energy cascades in which the total number of particles is immense but fluctuations are small.

The first nonstochastic numerical method was developed by Kalmykov and Chistjakov [28] for the fluctuations of the number of particle in nuclear cascade in the atmosphere. This method used the matrix representation of integral operators in ad-

joint equations. It was proposed that the functions are constant in each interval in which the energy axis was divided. We improved this method inserting the interpolation polynomials in these intervals. Our numerical method was described in works [29–33]. We have applied it to various problems of the cascade theory since 1977 (see Sec. 5,6).

4. Adjoint equation in fluctuation problems

Before some explicit forms of the adjoint equations will be described it is necessary to make some remarks. First of all we remind that the variable x contains a discrete component — the kind of particle α : $x = (\mathbf{y}, \alpha)$, where \mathbf{y} is a continuous component of x . Therefore

$$\int dx \equiv \sum_{\alpha} \int d\mathbf{y}, \quad \dot{x} \frac{\partial}{\partial x} = \dot{\mathbf{y}} \frac{\partial}{\partial \mathbf{y}}$$

because the latter is calculated by assumption that the collisions are absent. Secondly we note that the Markovian time may be either usual physical time (in nonstationary problems) or another continuous variable (for example the depth of a matter in one-dimensional stationary cascade problems). At last we suppose that the random value $q = q(x)$ has a continuous, even a differentiable density $\psi(q|x)$. The equations for the moments $\bar{q}^n(x)$ do not depend on the character of the density and the equation for the density itself is easily transformed into equation for a discrete random value.

In order to write an equation for the density of probability $\psi(q|x)$ we must have a full description of the detector property. If we deal with additive detector it is enough to know the response of the detector to one single particle. We denote the response to a free (without collisions) moving particle for a time dt by $a(x)dt$ and the response to the collision ($x \rightarrow x_1, \dots, x_k$) by $b_k(x \rightarrow x_1, \dots, x_k)$. Besides we introduce multiparticle exclusive distributions $v_k(x \rightarrow x_1, \dots, x_k)$ and inclusive distributions $\omega_k(x \rightarrow x_1, \dots, x_k)$ for the particles produced by a single particle at a point x per unit Markovian time. Finally we have

$$\begin{aligned} & \left[d^+ + \sigma + a \frac{\partial}{\partial q} \right] \psi(q|x) = v_0(x) \delta[q - b_0(x)] + \\ & + \sum_{k>0} \frac{1}{k!} \int dx_1 \cdots \int dx_k v_k(x \rightarrow x_1, \dots, x_k) \times \\ & \quad \times \psi(q|x_1, t) * \cdots * \psi(q|x_k, t) * \cdots \\ & \quad \cdots * [q - b_k(x \rightarrow x_1, \dots, x_k)]. \end{aligned} \quad (20)$$

Here $d^+ \equiv -\partial/\partial t - \dot{x}\partial/\partial x$, σ is a cross-section of interaction of the particle with a matter (per unit

of time), $v_0(x)$ is the probability of absorption of a particle in matter per unit of time, $b_0(x)$ is the response of a detector to this event and $*$ is the convolution sign:

$$\psi(q|1) * \psi(q|2) \equiv \int \psi(q'|1) \psi(q - q'|2) dq'.$$

Equations for the moments $\bar{q}^n(x)$ follow from the above equation (20):

$$\begin{aligned} & [d^+ + \sigma] \bar{q}^n(x) - \int dx' \omega_1(x \rightarrow x') \times \\ & \quad \times \bar{q}^n(x', t) = d^{(n)}(x). \end{aligned} \quad (21)$$

Here

$$d^{(1)}(x) = a(x) + \sigma(x) \bar{b}(x)$$

and

$$\begin{aligned} d^{(2)} &= 2a(x) \bar{q}(x) + \sigma(x) \bar{b}^2(x) + \\ & \quad + 2 \int dx' c(x \rightarrow x') \bar{q}(x', t) + \\ & \quad + \int dx' \int dx'' \omega_2(x \rightarrow x', x'') \bar{q}(x', t) \bar{q}(x'', t). \end{aligned}$$

Besides

$$\begin{aligned} \bar{b}(x) &= \sum_{k>0} \frac{1}{k!} \int dx_1 \cdots \int dx_k \times \\ & \quad \times v_k(x \rightarrow x_1, \dots, x_k) b_k(x \rightarrow x_1, \dots, x_k), \end{aligned}$$

and

$$\begin{aligned} c(x \rightarrow x') &= v_1(x \rightarrow x') b_1(x \rightarrow x') + \\ & + \sum_{k>0} \frac{1}{k!} \int dx_1 \cdots \int dx_k v_{k+1}(x \rightarrow x_1, \dots, x_k, x') \times \\ & \quad \times b_{k+1}(x \rightarrow x_1, \dots, x_k, x'). \end{aligned}$$

These equations were obtained and analyzed in our works [9,10,34]. Lately we have derived the equation for the variance

$$D(x) \equiv \mathbf{D}q(x) = \bar{q}^2(x) - \bar{q}^2(x)$$

immediately. It was shown also that the variance may be decomposed into two components by two ways:

$$D(x) = D^{(1)}(x) + D^{(2)}(x) = D_1(x) + D_2(x)$$

The components obey the equations

$$[d^+ + \sigma] D^{(i)}(x) = B^{(i)}, \quad (22)$$

and

$$\begin{aligned} & [d^+ + \sigma] D_i(x) - \\ & - \int dx' \omega_1(x \rightarrow x') D_i(x', t) = B_i(x), \end{aligned} \quad (23)$$

where

$$B^{(1)}(x) = B_1(x) = \frac{1}{\sigma(x)}[a(x) - d^+\bar{q}(x)]^2,$$

$$B^{(2)}(x) = \sigma(x)D'(x), \quad B_2(x) = \sigma(x)D''(x),$$

$$D'(x) = \mathbf{D}[b_\nu(x \rightarrow x_1, \dots, x_\nu) + \sum_{i=1}^{\nu} q(x_i, t)]$$

and

$$D''(x) = \mathbf{D}[b_\nu(x \rightarrow x_1, \dots, x_\nu) + \sum_{i=1}^{\nu} \bar{q}(x_i, t)].$$

The meanings of the components are different for the different ways of the decomposition.

$D^{(1)}(x)$ is the component part of the variance brought by the fluctuations of the first free path of primary particle only;

$D^{(2)}(x)$ is the component part of the variance brought by the fluctuations of remaining free paths and random distributions of produced particles in x -space;

$D_1(x)$ is the component part of the variance brought by the fluctuations of all free paths of particles;

$D_2(x)$ is another component part brought by the fluctuations in random distributions of secondary particles produced in elementary events;

$D'(x)$ is the variance in cascade with fixed point of the first collision of primary particle;

$D''(x)$ is the part of the latter generated in the first collision because of fluctuations of random distribution of secondary particles only.

The components D_2 and $D^{(2)}$ may be decomposed then into the parts generated in elementary processes of different kinds.

This approach was extended on the covariance function for a set of detectors:

$$c_{ij}(x) = cov(q_i(x), q_j(x)) = \bar{q}_i \bar{q}_j(x) - \bar{q}_i \bar{q}_j(x).$$

Let t be a longitudinal co-ordinate in one-dimensional problem and A be a region in the x -space. The number of particles belonging to A in a depth t' as a function of $t' - t$

$$N(x, t; A, t') \equiv N(x, t' - t)$$

is called the individual (random) cascade curve. As it was shown in the work [35] the longitudinal moments

$$N^{(k)}(x) = \int_0^\infty N(x, \tau) \tau^k d\tau, \quad (24)$$

are very significant for description of individual cascade of high energy in homogeneous media. We

have derived equations for the mean values $\bar{N}^{(k)}(x)$ and the covariance matrix

$$C_{kl}(x) \equiv cov(N^{(k)}(x), N^{(l)}(x))$$

of the random moments. They are of the form:

$$[-\dot{x} \frac{\partial}{\partial x} + \sigma] \bar{N}^{(k)}(x) - \int dx' \omega_1(x \rightarrow x') \bar{N}^{(k)}(x') = k \bar{N}^{(k-1)}(x) + 1(x, A) \delta_{k0}, \quad (25)$$

$$[-\dot{x} \frac{\partial}{\partial x} + \sigma] C_{kl}(x) - \int dx' \omega_1(x \rightarrow x') C_{kl}(x') = (1/\sigma(x)) [1(x, A) \delta_{k0} + \dot{x} \frac{\partial \bar{N}^{(k)}}{\partial x}] \times$$

$$\times \left[1(x, A) \delta_{l0} + \dot{x} \frac{\partial \bar{N}^{(l)}}{\partial x} \right] + k C_{k-1, l}(x) + l C_{k, l-1}(x) + \sigma(x) C''_{kl}(x), \quad (26)$$

here

$$C''_{kl}(x) = cov \left(\sum_{i=1}^{\nu} \bar{N}^{(k)}(x_i), \sum_{j=1}^{\nu} \bar{N}^{(l)}(x_j) \right),$$

$$1(x, A) = \begin{cases} 1, & x \in A, \\ 0, & x \notin A. \end{cases}$$

We have derived also equations for the lateral moments of random distribution of particles in a fixed depth in frame of small-angle approximation.

5. Numerical method of solution of adjoint equations

Since most problems of interest described by the adjoint equations (8)–(15), (21)–(23) are not amenable to analytical solutions, a numerical method must be used to compute detector reading Q . Such method was developed in our papers [29–33]. Here, a short review of this method is useful for a more comprehensive statement of the problem.

Let us represent one-dimensional adjoint equation in the form

$$\frac{\partial q}{\partial t} + \sigma q - \int_{E_{th}}^E dE' w(E \rightarrow E') q(t, E') = F, \quad (27)$$

where q is the adjoint function, E is the energy of a primary particle, $t = z^* - z$ is the distance between a primary particle and plane, where boundary conditions are defined, σ is cross-section of interaction of particle, $w(E \rightarrow E')$ is differential cross-section

of elementary process, F is function defined by conditions of the problem.

Introduce the increasing sequence $E_0 = E_{th}, E_1, \dots, E_k, \dots$ on the energy axis and the definitions $q_k(t) = q(t, E_k)$, $\sigma_k = \sigma(E_k)$, $F_k(t) = F(t, E_k)$. Consider the integral

$$\begin{aligned} I_k &= \int_{E_{th}}^{E_k} dE' w(E_k \rightarrow E') q(t, E') = \\ &= \sum_{i=1}^k \int_{E_{i-1}}^{E_i} dE' w(E_k \rightarrow E') q(t, E') = \sum_{i=1}^k I_{ki} \quad (28) \end{aligned}$$

and approximate $q(t, E)$ on each segment $[E_{i-1}, E_i]$ by the Lagrange interpolation polynomial the choice of power n of which and nodes of the interpolation is made as follows. The maximum power of used polynomials \mathcal{N} is defined; for segments with the number i , $\mathcal{N} \leq i \leq k$, the maximum power polynomials with nodes $E_{i-\mathcal{N}}, \dots, E_i$ are used, points $E_0, E_1, \dots, E_{\mathcal{N}}$ are used for segments with the number $i < \mathcal{N}$ if $k \geq \mathcal{N}$, otherwise the power of the interpolation polynomial falls to k , and points E_0, E_1, \dots, E_k are considered to be the nodes.

Thus, the power of the interpolation polynomial n and the number of the extreme right point of interpolation m for $[E_{i-1}, E_i]$ is defined by the formulas

$$n(k, i) = \min\{k, \mathcal{N}\}, \quad m(k, i) = \begin{cases} n(k, i), & i < \mathcal{N}, \\ i, & i \geq \mathcal{N}, \end{cases}$$

then

$$q(t, E) = \sum_{j=m-n}^m L_{ij}^n(E) q_j(t), \quad (29)$$

where

$$L_{ij}^n(E) = \prod_{\substack{r=0 \\ r \neq m-j}}^n \frac{E - E_{m-r}}{E_j - E_{m-r}}, \quad E \in \Delta E_i.$$

Substituting (29) into (28) and interchanging the order of summation we shall get:

$$I_{ki}(t) = \sum_{j=m-n}^m \Delta_{kij} q_j(t), \quad (30)$$

where

$$\Delta_{kij} = \int_{E_{i-1}}^{E_i} dE' w(E_k \rightarrow E') L_{ij}^n(E').$$

Let us set $E = E_k$ in the equation (27) and apply the expansion (30) for integral part of this equation. As a result we shall have:

$$\frac{\partial q_k}{\partial t} + A_k(t) q_k(t) = F'_k(t), \quad (31)$$

where

$$\begin{aligned} A_k(t) &= \sigma_k - a_{kk}, \\ F'_k(t) &= F_k(t) + \sum_{j=0}^{k-1} a_{kj} q_j(t), \\ a_{kj} &= \sum_{i=1}^k \Delta_{kij} \sum_{s=m-n}^m \delta_{sj}. \end{aligned}$$

Introduce still the sequence $t_0, t_1, \dots, t_l, \dots$ and let $\Delta t = t_l - t_{l-1}$, $q_{k,l} \equiv q_k(t_l)$. For each of intervals (t_{l-1}, t_l) one can put down the solution of equation (31), considering $q_{k,l-1}$ as boundary conditions. Suppose $t = t_l$, we shall get

$$\begin{aligned} q_{k,l} &= q_{k,l-1} \exp \left\{ - \int_{t_{l-1}}^{t_l} A_k(t') dt' \right\} + \\ &+ \int_{t_{l-1}}^{t_l} F'_k(t') \exp \left\{ - \int_{t'}^{t_l} A_k(t'') dt'' \right\} dt'. \quad (32) \end{aligned}$$

Thus, we come to the following scheme of solution of adjoint equation (27). Using boundary condition $q_{0,0}$ and right part $F'_0(t) = F_0(t)$ according to the formula (32) we find the value $q_{0,l}$ for l from 1 to some value l_0 . Setting then $k = 1$ in (32) and using previously found value $q_{0,l}$ we shall have $q_{1,l}$ for the same range of changing l . Having repeated this procedure till $k = k_{\max}$, we come back again to $k = 0$ and construct the solution analogically in the region $l_{0+1} \leq l \leq 2l_0$, using q_{k,l_0} as boundary conditions, etc. Integration over t in the formula (32) can be taken out approximating functions to be integrated by polynomials of the same power l_0 .

The accuracy and time of calculations by the method mentioned above are defined by the quantities of parameters $\Delta t, \varepsilon = E_i/E_{i-1}, \mathcal{N}, l_0$. We find the optimal values of these quantities by making test calculations. It has been found that it is enough to choose $\varepsilon = 10^{1/12} \div 10^{1/16}$ for reaching the accuracy of several percents. In this case polynomials with $\mathcal{N} \geq 2$ satisfactorily describe the energy dependence of solution. We set $l_0 = 4$ and the values Δt were changed from $\Delta t \sim 10^{-3}$ for $t \leq 1$ until 0.25 after the maximum of the shower (in radiation units).

Note, that the convergence of this numerical method was proved in our paper [36].

6. Cascade characteristics

It is impossible to discuss in journal article all essential results of our calculations. For this reason we only present here limited number of results to demonstrate the usefulness and importance of adjoint formalism in cosmic ray problems.

Electromagnetic cascade characteristics

The cycle of calculations of electromagnetic shower parameters for a series of materials ($6 \leq z \leq 82$) in the extensive range of threshold ($10^5 \div 10^8$ eV) and primary (until 10^{20} eV) energies was carried out by this method. Cascade curves, the range and dissipated energy in the finite layer, the Čerenkov radiation, the angular and radial distribution of electrons and other quantities were calculated [14,29–31,37–41]. These results are in good agreement with experimental data, the Monte Carlo calculations and also with calculations based on the numerical solution of basic cascade equations. The Table 1 demonstrates the calculations performed within the framework of the adjoint approach. Some of them are also presented in Fig. 1,2,3,4.

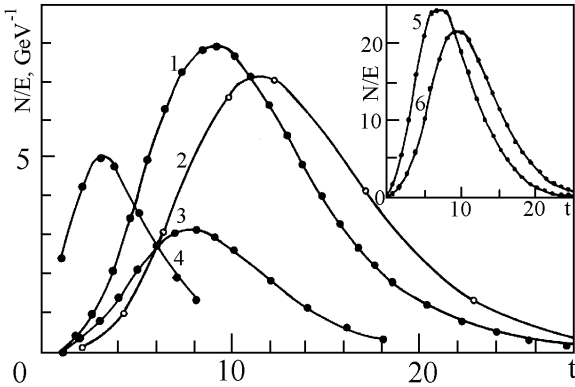


Figure 1. Cascade curves of electrons in lead (1–4) and iron (5–6) for showers generated by primary electrons. $E_{th} - E$ (eV): 10^6-10^{11} (1), 10^6-10^{12} (2), 10^7-10^{11} (3), 10^7-10^9 (4), 10^6-10^{10} (5), 10^6-10^{11} (6), \bullet — data [45], \circ — data [46], — — our calculation [31]

Here our data on electromagnetic cascade characteristics in the air will be presented. They are of interest in the analysis of extensive air showers.

1. The analysis of the results has shown that in the region $E_{th} \leq 0.25$ MeV the cascade curves

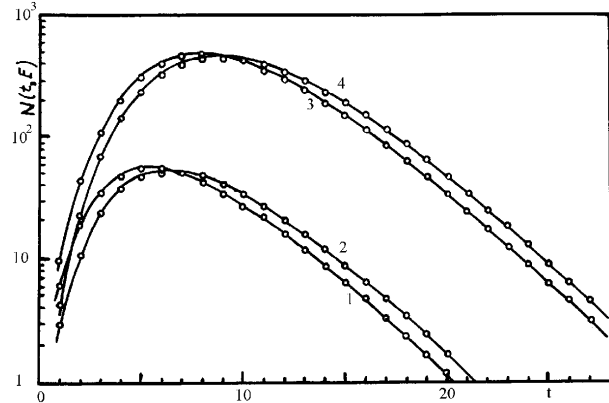


Figure 2. Cascade curves of electrons in iron for showers generated by electrons (1,3) and photons (2,4). $E = 10^{10}$ eV (1,2), $E = 10^{11}$ eV (3,4). \circ — data [45] ($E_{th} = 0.316 \cdot 10^6$ eV), — — our calculation ($E_{th} = 0.316 \cdot 10^6$ eV)

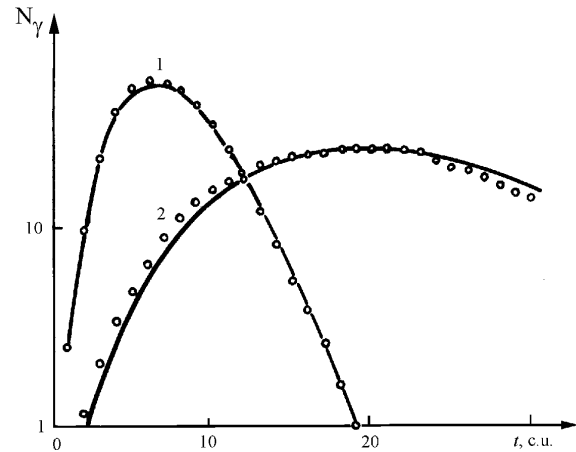


Figure 3. Cascade curves in lead in photon-initiating electromagnetic cascade without and with Landau-Pomeranchuk-Migdal (LPM) effect. $E = 10^6$ GeV, $E_{th} = 10^3$ GeV: 1 — without LPM effect, 2 — with LPM effect, \circ — [48], — — our calculations

and \bar{r}^2 in homogeneous atmosphere practically do not depend on E_{th} [14]; their changes under the decrease of E_{th} from 0.25 MeV to 0.1 MeV are not higher than 2%. According to these facts which agree with the conclusion [46], the data for $E_{th} = 0.1$ MeV can be considered as the characteristics of the total number of cascade particles ($E_{th} = 0$).

2. The total number of shower electrons of energies greater than zero in photon-initiating cascade was approximated with using Greisen's formula,

$$N_G(t, E) = \frac{0.31}{\sqrt{\ln(E/\beta)}} \exp\left\{\left(1 - \frac{3}{2} \ln s\right)t\right\},$$

Table 1

Test calculations

Shower characteristic	Medium	Primary energy, GeV	Threshold energy, MeV	Method
Track length of electrons in infinite medium	Lead	0.1-1	1	Monte Carlo(MC) [42]
	Lead Xenon	0.15–0.55 0.025–1	5 3.066	experiment [43] MC [44]
Cascade curve	Lead	$1-10^3$	1;10	Multigroup [45]
	Lead	10^3	1	Multigroup [46]
	Lead	6	10	MC [47]
	Lead	10^6	10^6	MC [48,49]
	Iron	$10; 10^2$	0.3;1	Multigroup [45]
	Air	$10; 10^2$	0.316	Multigroup [45]
	Air	10	0.1–4	MC [50]
	Air	$10; 10^2$	0;4	MC [51,52]
	Air	$10-10^6$	0	Semi-analytical MC [53]
Čerenkov radiation	Air	1-300		MC [54]
Track length of electrons in finite layer	Xenon	1	3.066	MC [44]
Sum of the number of electrons at different depths ($s = \sum_i N(t_i)$)	Lead	2–15	0.5	experiment [55]
	Xenon	1.5	1.5	experiment [56]
Angular distribution of electrons	Air	10	1	MC [50]
	Air	$10-10^5$	25–80	Semi-analytical MC [37]
$\sqrt{r^2}$	Air	10	4	MC [51]
	Air	10	0.1;0.4	MC [50]
Radial distribution of electrons	Air	$10; 10^2$	0	MC [51]
	Air	10	0.25;4	MC [50]
	Air	10^3	0	MC [57]
	Air	$10-10^6$	0	Semi-analytical MC [58]

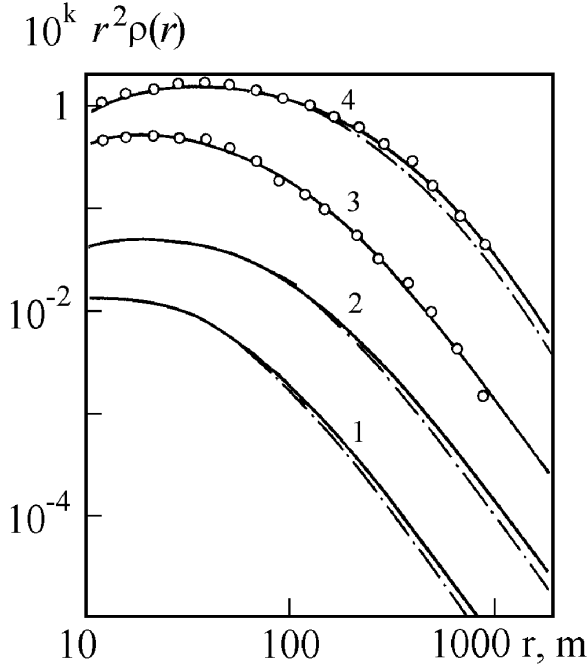


Figure 4. Radial distribution of the total number of electrons in the air showers [40]. $E_\gamma = 10^5$ GeV:
 1 — $s = 0.63$, $k = -0.5$;
 2 — $s = 1$, $k = 0$;
 3 — $s = 1$, $k = 1$;
 4 — $s = 1.4$, $k = 1.5$.
 ○ — data of the semi-analytical Monte Carlo method;

—, — — — — data of the method for solving the adjoint equations with and without taking account of the deflection of photons in Compton scattering process, respectively

$$s = \frac{3t}{t + 2\ln(E/\beta)},$$

in the following way:

$$N_\gamma(t, E) = \gamma(t, E)N_G(t, E).$$

Correction factor $\gamma(t, E)$ presented in Table 2 ($t_0 = 36.1$ g/cm², $\beta = 81$ MeV) gives information about accuracy of Greisen's formula in high energy region.

3. The angular distribution of electrons $\rho(\theta; E, E_{th}, s)$ and the mean square angles $\theta_{m.s.a.}$ in the air showers have been obtained. The analysis of these results has shown that the distribution of the electrons as a function of the variable $x = \theta/\theta_{m.s.a.}$ in the region $0.05 \leq x \leq 5$ does not depend practically on the primary and threshold energies and depends only on the shower age parameter s [37]:

$$\rho(\theta; E, E_{th}, s)\theta d\theta = \rho_\theta(x; s)xdx. \quad (33)$$

Table 2

Correction factor $\gamma(t, E)$ [39]

t , rad. units	Primary photon energy, GeV						
	10	10 ²	10 ³	10 ⁴	10 ⁵	10 ⁶	10 ⁷
1	1.02	1.01	1.06	1.14	1.24	1.35	1.47
2	1.06	1.04	1.07	1.13	1.22	1.32	1.45
4	1.09	1.06	1.05	1.06	1.12	1.19	1.28
6	1.10	1.06	1.03	1.02	1.07	1.11	1.16
8	1.15	1.08	1.04	1.01	1.05	1.06	1.09
10	1.20	1.11	1.05	1.01	1.04	1.02	1.06
12	1.36	1.18	1.09	1.03	1.05	1.04	1.04
14	1.56	1.28	1.15	1.07	1.06	1.05	1.04
16	1.76	1.39	1.21	1.11	1.09	1.07	1.04
18	2.06	1.52	1.29	1.19	1.13	1.09	1.06
20	2.40	1.70	1.41	1.25	1.18	1.12	1.09
22	2.81	1.92	1.56	1.33	1.24	1.17	1.11
24	3.32	2.22	1.72	1.44	1.30	1.22	1.16
26	3.93	2.54	1.91	1.57	1.38	1.28	1.21
28	4.65	2.92	2.14	1.72	1.48	1.35	1.26

Table 3

Angular distribution function of electrons $\rho_\theta(x; s)$, $x = \theta/\theta_{m.s.a.}$ [9]

x	$s = 0.6$	$s = 1.0$	$s = 1.4$
0.05	$3.53 \cdot 10^{-1}$	$2.10 \cdot 10^{-1}$	$1.68 \cdot 10^{-1}$
0.1	$2.53 \cdot 10^{-1}$	$2.10 \cdot 10^{-1}$	$1.81 \cdot 10^{-1}$
0.2	$1.56 \cdot 10^{-1}$	$1.75 \cdot 10^{-1}$	$1.70 \cdot 10^{-1}$
0.5	$9.70 \cdot 10^{-2}$	$1.08 \cdot 10^{-1}$	$1.35 \cdot 10^{-1}$
1	$3.67 \cdot 10^{-2}$	$5.32 \cdot 10^{-2}$	$6.41 \cdot 10^{-2}$
2	$1.08 \cdot 10^{-2}$	$1.00 \cdot 10^{-2}$	$1.35 \cdot 10^{-2}$
3	$3.81 \cdot 10^{-3}$	$2.44 \cdot 10^{-3}$	$2.83 \cdot 10^{-3}$
4	$1.35 \cdot 10^{-3}$	$6.41 \cdot 10^{-4}$	$3.81 \cdot 10^{-4}$
5	$3.29 \cdot 10^{-4}$	$1.68 \cdot 10^{-4}$	$1.03 \cdot 10^{-4}$

The function $\rho_\theta(x; s)$ is given in Table 3.

4. The lateral distribution function (LDF) of the total number of electrons in the air showers has been obtained for the primary energies 10^{10} – 10^{15} eV. The results of our calculations were described by modified NKG-formula [14]

$$\rho(r) = (mr_M)^{-2} \rho^{NKG} \left(\frac{r}{mr_M} \right),$$

$$r_M = 80 \text{ m},$$

where $m \approx 0.78 - 0.21s$ for $0.6 \leq s \leq 1.6$ and $0.5 \leq r \leq 200$ m.

Note that later these results were confirmed by the Monte Carlo simulations [57] for primary energy $E_\gamma = 10^3$ GeV and the semi-analytical Monte Carlo calculations for $E_\gamma \leq 10^7$ GeV [59].

To obtain correct results at large distance from shower axis it is necessary to take into account the deflection of photons in Compton scattering process [57,59]. The Monte Carlo simulations [59] showed that cancelling of photon deflections leads to large underestimations of electron flux density at $r > 300$ m. Therefore, the deflection of photons in Compton scattering process (in the small angle approximation) was included into equation (11); a very good agreement with Monte Carlo results was obtained (see Fig.4) [40]. This demonstrated the validity of the small angle approximation and allowed us to calculate the LDF of electrons in air showers in the region of distances from axis up to 2000 m [40,41].

5. To analyse the dependence of the LDF on the energy E_γ and cascade age s in recent paper, we use the variable $x = r/r_{m.s.r.}$ [38], where $r_{m.s.r.}(E, s)$ is the mean square radius of the shower

$$r_{m.s.r.}(E, s) = \left[2\pi \int_0^\infty r^2 f(r, E, s) r dr \right]^{1/2}.$$

The lateral distribution $f(x, E, s)$ with respect to x is related with $f(r, E, s)$ by the formula

$$x f(x, E, s) = r_{m.s.r.} r f(r, E, s).$$

This distribution function is normalized as

$$2\pi \int_0^\infty x f(x, E, s) dx = 1.$$

Detailed analysis of the calculational data in [60] allows us to conclude that distribution $x f(x, E, s)$ as a function of the variable x in the region $0.05 \leq x \leq 25$ does not depend practically on the primary energy E and the shower age parameter s :

$$x f(x, E, s) \approx x f(x).$$

This new scaling property on the lateral distribution is illustrated in Fig. 5. We approximate $x f(x)$ as

$$x f(x) = \exp(-3.63 - 1.89 \ln x - 0.370 \ln^2 x - 0.0168 \ln^3 x). \quad (34)$$

Our fitting function is also shown in Fig. 5. In Table 4 we present the range of variation of r corresponding to the region $0.05 \leq x \leq 25$.

Table 4
Data on the $r = x r_{m.s.r.}$ (m) for minimum and maximum values of x considered in our paper. $E_\gamma = 10^8$ GeV

x	s				
	0.6	0.8	1.0	1.2	1.4
0.05	1.7	2.4	3.5	5.2	7.7
25	830	1210	1770	2600	3860

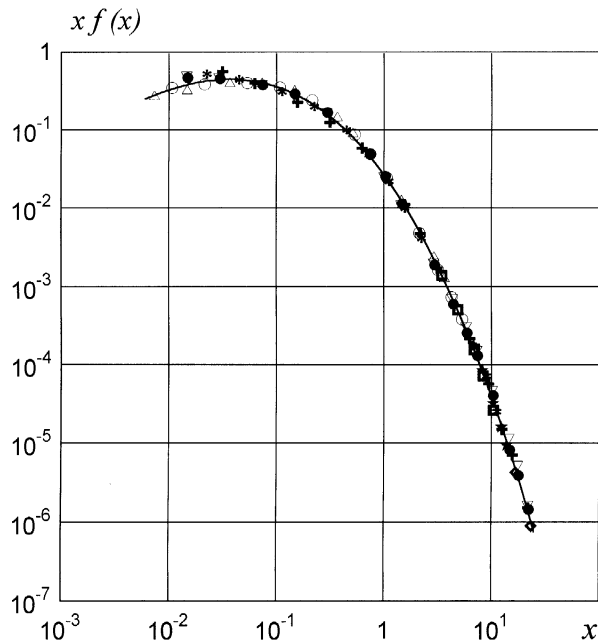


Figure 5. The dependence of the invariant part of the LDF of electrons on the scaling variable $x = r/r_{m.s.r.}(E, s)$.

$\diamond - E_\gamma = 10^2$ GeV, $s = 0.6$; $+ - E_\gamma = 10^5$ GeV, $s = 0.6$;
 $* - E_\gamma = 10^4$ GeV, $s = 0.8$; $\bullet - E_\gamma = 10^5$ GeV, $s = 1.0$;
 $\nabla - E_\gamma = 10^9$ GeV, $s = 1.0$; $\circ - E_\gamma = 10^4$ GeV, $s = 1.2$;
 $\triangle - E_\gamma = 10^4$ GeV, $s = 1.4$; $\square - E_\gamma = 10^5$ GeV, $s = 1.4$;
 $\star - E_\gamma = 10^6$ GeV, $s = 1.4$.

The solid curve is from our fitting function (34).

Thus, the electron lateral distribution $r f(r, E, s)$ in the radial region $x \geq 0.05$ is well described by the formula [61]

$$r f(r, E, s) = \frac{x f(x)}{r_{m.s.r.}(E, s)},$$

where $x f(x)$ is given by (34) and

$$r_{m.s.r.}(E, s) = 296 \exp\{-3.69 + 0.0505 \ln E - 0.00175 \ln^2 E + s [1.81 + 0.00638 \ln E - 0.0826 / \ln E]\}, \text{ m,}$$

for $s = (0.5 \div 1.6)$ and $E_\gamma = (10 \div 10^9)$ GeV. The electron density Δ can be calculated from the function $f(r, E, s)$ by $\Delta =$

$N(t, E)f(r, E, s)$, where $N(t, E)$ is the total number of electrons at the observation level in photon-initiated cascade.

EAS characteristics

The calculations of different EAS characteristics were performed in the model of quark-gluon strings [62]. The cascade curves, radial distribution of electrons, lateral distribution of Čerenkov radiation and other characteristics were obtained. Extensive numerical comparisons were performed between our results and experiment data [33,39,63]. Some our results are presented in Fig.6, 7, 8. In particular, we obtain the agreement with the data assuming that 29–34% of primary cosmic rays consist of an iron nuclei at energies 10^6 – 10^7 eV and primary photons prevail at energies higher than 10^8 GeV [39].

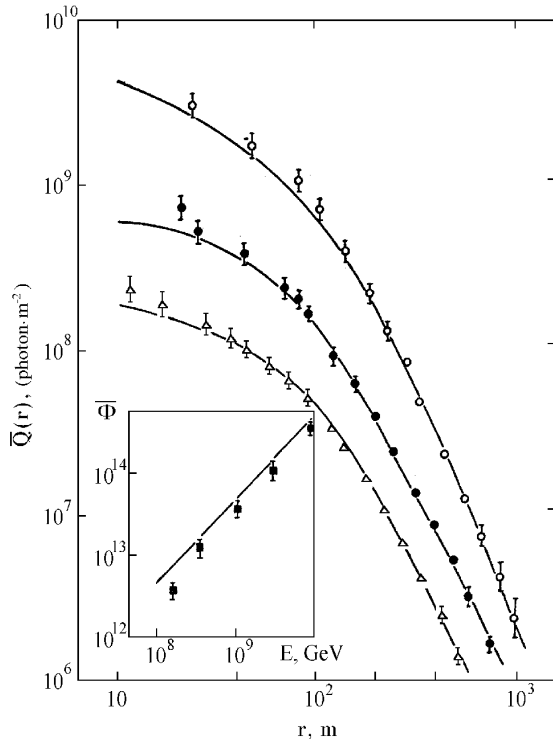


Figure 6. Lateral distribution of Čerenkov radiation at sea level with the number of light quanta \bar{f} . Δ — $\bar{f} = 8.9 \cdot 10^{12}$ quanta, \bullet — $\bar{f} = 2.66 \cdot 10^{13}$ quanta, \circ — $\bar{f} = 1.2 \cdot 10^{14}$ quanta [64], — — our calculations [39]

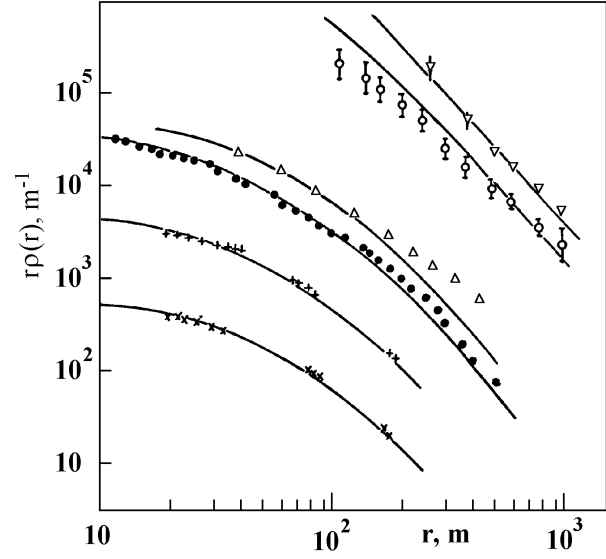


Figure 7. Radial distribution of EAS electrons. $\times, +$ — data [65] ($z^* = 700 \text{ g/cm}^2, \theta \leq 30^\circ, \times - N_e = 1.79 \cdot 10^5, + - N_e = 1.44 \cdot 10^6$); \bullet — data [66] ($z^* = 930 \text{ g/cm}^2, \theta \leq 30^\circ, N_e = 10^7$); Δ — data [67] (sea level, $\theta \leq 30^\circ, N_e = 2 \cdot 10^7$); \circ, ∇ — data [68] (sea level, $\rho_{600} = 11$ and $26.3 \text{ m}^{-2}, \theta = 17^\circ$ and 22°); — — our calculations [39]

Muon transport in rock

The interpretation of measurements of deep underground experiments is based on the theoretical data for muon survival probability and depth-intensity relations. This is a reason which during long time stimulated the theoretical investigations in the problem of the propagation of high energy muons through thick layers of materials. Over the last 30 years the problem of muon transport in rock has been solved by various authors by means of analytical, semi-analytical and Monte Carlo methods (see, for example, [3,73–82]). In these calculations it was traditionally supposed that the fluctuations in bremsstrahlung and photonuclear interactions of muon played the main role. The energy loss fluctuations in knock-on electron and pair production were neglected. The energy losses in these processes were taken into account as continuous.

In our works [83,84] we have also considered this problem within the framework of adjoint approach. However we have taken into account the energy loss fluctuations due to knock-on electron and pair production. The survival probability $P(z, E)$ was found by the numerical solution of adjoint equation (15). The differential cross sections of elementary processes have been described by well-known formulas [2,85–87].

In order to analyse the influence of energy loss

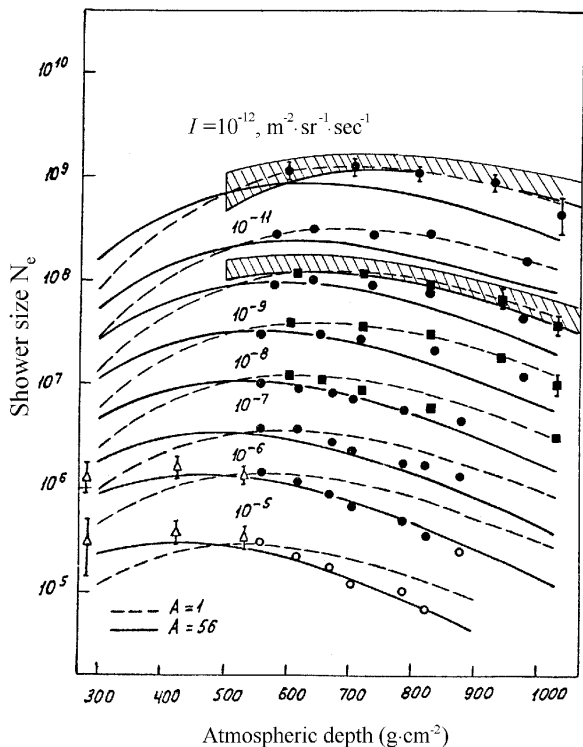


Figure 8. Equi-intensity curves of EAS electrons:
 \circ, \bullet, \square — data from [69,70],
 Δ — data [71,72],
 hatched — [64],
 — — — — — our calculations [39]

fluctuations in knock-on electron and pair production on the vertical muon intensity approximate results $\tilde{P}(z, E)$ were obtained by solution of equation

$$-\frac{\partial \tilde{P}(z, E)}{\partial z} + (\beta_i + \beta_p) \frac{\partial \tilde{P}(z, E)}{\partial E} + \tilde{\sigma}_\mu \tilde{P}(z, E) - \sum_{\beta=b,n} \int dE' w_{\mu\beta}(E \rightarrow E') \tilde{P}(z, E - E') = \delta(z - z^*) \varepsilon(E - E_{th}),$$

$$\tilde{\sigma}_\mu = \sum_{\beta=b,n} \int dE' w_{\mu\beta}(E \rightarrow E').$$

The vertical muon intensity $J(z^*, E_{th})$ which is the observable value in deep underground experiments is related to $P(z, E)$ and muon energy differential spectrum at sea level $s_\mu(E)$ by the relation (6). We have

$$J(z^*, E_{th}) = \int_{E_{th}}^{\infty} dE' s_\mu(E') P(z = 0, E'),$$

$$\tilde{J}(z^*, E_{th}) = \int_{E_{th}}^{\infty} dE' s_\mu(E') \tilde{P}(z = 0, E').$$

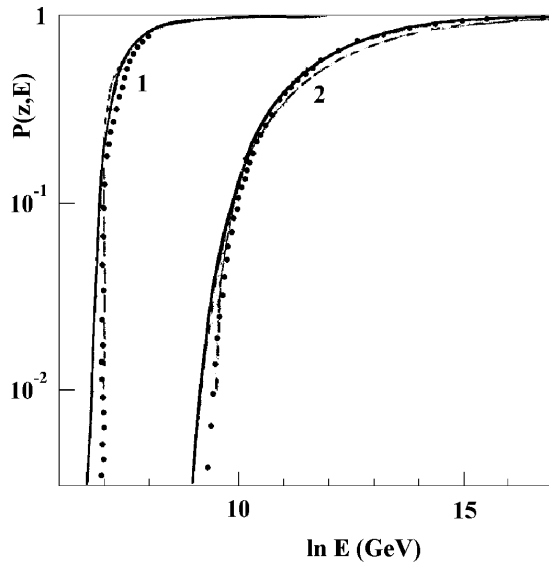


Figure 9. Survival probability of muon in standard rock:

1 — $z^* = 3.1$ km w.e., 2 — $z^* = 10.1$ km w.e.;
 — — — — — our exact results [84], $\bullet\bullet\bullet$, — — — — — results obtained without taking account of the energy loss fluctuations due to knock-on electron and pair production;
 $\bullet\bullet\bullet$ — our data [84], — — — — — data [81]

The influence of the energy loss fluctuations due to knock-on electron and pair production on the survival probability and vertical muon intensity at the large depths are shown in Fig.9. It is seen that taking account of these fluctuations results in increase the vertical muon intensity at the large depths. This result is clear since, as a consequence of the steepness of the muon spectrum at sea level, a large fraction of the underground muon response is produced by muons with small P .

7. The fluctuations of EMC

The number of electrons with energy over E_{th} in a fixed distance from a point of birth of a primary particle

This statement of problem is traditional one for the cascade theory, from which the theory began. The adjoint equations (21) were calculated numerically for the threshold energies from 0.1 to 1 MeV in the primary energy region $1 \div 10^6$ GeV for EMC in air, iron and lead [88]. The results were compared with those of other authors, obtained by means of analytical methods, Monte Carlo technique and experiments. The comparison has shown that the numerical results coincide with Monte Carlo and experiment data but differ from analytical results

The example of correlation matrix ($E_\gamma = 10^4$ GeV)

t	2	4	6	8	10	12	14	16	18	20
2	1	0.93	0.82	0.68	0.48	0.06	-0.65	-0.68	-0.59	-0.50
4		1	0.96	0.85	0.65	0.17	-0.75	-0.85	-0.76	-0.67
6			1	0.96	0.81	0.32	-0.76	-0.96	-0.89	-0.81
8				1	0.94	0.54	-0.64	-0.99	-0.98	-0.92
10					1	0.79	-0.36	-0.92	-0.99	-0.99
12						1	0.27	-0.48	-0.76	-0.89
14							1	0.71	0.41	0.20
16								1	0.93	0.82
18									1	0.97
20										1

A- and B-approximations. The difference between the analytical and numerical results is about 20–40 %, because of the rough account of low energy processes by analytical approximations, of cross-sections.

It has turned out that the dependence of the fluctuation on the depth has a simple approximation. In particular we have for electrons with $E_{th} > 1$ MeV in air from primary photon with energy $E \in [10^3, 10^6]$ GeV in the region $t \in [0.3t_{max}, 2t_{max}]$ the following approximation:

$$\delta_N^2(t) \approx (1 - t/t_{min})^2, \\ t_{min} \approx t_{min} + 1(r.l.),$$

where t_{max} is the depth of maximum of mean cascade curve. This formula is not accurate about t_{max} , but fluctuations are small here. The more accurate approximation of numerical results leads to the following remarkable formula for fluctuations at the point t_{max} :

$$\delta_N^2(t_{max}) = 0.12\bar{N}_m^{-1/4} + \bar{N}_m^{-1} \quad (35)$$

where $N_m = \bar{N}(t_{max})$ is the maximum of the mean cascade curve. The representation (35) is obtained by analysing fluctuations of EMG in air ($E_{th} = 25$ MeV), iron and lead ($E_{th} = 1$ MeV) in the region $N_m \in [10, 10^5]$

The depth correlations of the electron number fluctuations

There were calculated depth correlation matrixes for numbers of electrons in EMC in air for incident energies from 10 GeV to 10^5 GeV [89].

$$k(t_1, t_2) = cov(N(t_1), N(t_2))[\mathbf{DN}(t_1)\mathbf{DN}(t_2)]^{-1/2}.$$

The behavior of the correlations with a change t_1 and t_2 (see Table 5) brings us to the idea that

the fluctuations of cascade curve as a whole have a random shift character. Later we'll return to this idea.

The total path of all cascade electrons and others characteristics

The analytical solution for the total path of all electrons with energy over E_{th} in cascade developed in infinite homogeneous medium from a primary particle with incident energy E was obtained in approximation A [90]:

$$\delta_R = 0.90(E/E_{th})^{-1/2}, \quad E \rightarrow \infty. \quad (36)$$

Monte-Carlo and experimental results have a similar form:

$$\delta_R = A(E_{th})(E/E_{th})^{-1/2}. \quad (37)$$

Our numerical calculations for xenon show that the asymptotic (37) reaches soon enough with growth of incident energy E : by $E = 10^2$ MeV if $E_{th} = 1$ MeV and much sooner if $E_{th} \geq 10$ MeV. However $A(E_{th})$ tends to its limiting value much slowly (see the Table 6). The difference between asymptotic behaviors (36) and (37) demonstrates the error of A-approximation because of rough account of a low energy interactions.

Fluctuations of the total number of all secondary electrons, ionization loss energy, Čerenkov radiation in infinite medium have the same asymptotics (36) [91]. But if we deal with the detector which sensitivity depends on coordinate, the asymptotic may be changed. It takes place for total-absorption scintillation spectrometers where effect of absorption of scintillation light is essential. Our calculations by random moment method (see

Table 6

The coefficient $A(E_{th})$.

E_{th}, MeV	1	10	50	∞
Lead	0.70	0.78	0.81	0.90
Xenon	0.65	0.77	0.81	0.90
Air	0.39	0.64	0.72	0.90

below) have shown that account of this effect leads to asymptotic $\delta = \text{const}E^{-1/4}$ [92] which agrees with experiment.

The simplest model of ionization calorimeter as based on the following formula for its reading:

$$s = \sum_i N(t_i)\Delta t_i,$$

where t_i indicates the positions of sensitive planes (thin ionization gaps or scintillation layers), Δt_i are distances between next planes. Analytical description of fluctuations of this value was given in work [93]. It was shown that

$$\delta_s^2(\Delta t) = \delta_R^2 + o(\Delta t), \quad \Delta t \rightarrow 0.$$

Lately we carried out numerical calculations for really calorimeter which reading may be represented by the sum

$$\delta^2 = \delta_s^2 + \delta_{scat}^2 + \delta_1^2/\bar{S}, \quad (38)$$

where Δ_{scat}^2 is responsible for the scattering and transition effects and the last term corresponds to fluctuations of signals from single electrons crossing the sensitive planes. All the terms are comparable by largeness [9].

The total path of all electrons in a thick homogeneous layer

We have obtained by analytical method [91] that for a thick layer

$$\delta_R(t)^2 = \delta_R(\infty)^2 + \left(\frac{\bar{N}(t)}{\lambda_1(s)\bar{R}(t)} \right)^2 \delta_N(t)^2, \quad (39)$$

where $N(t)$ is the number of electrons at the boundary of the layer, $\lambda_1(s)$ is a well-known cascade function and the saddle point s obeys the equation

$$t = \ln x/\lambda_1'(s),$$

$x = E_{th}/E$ in A-approximation or β/E in B-approximation. This result is affirmed by our numerical calculation. The relationship (36) may be easily explained by assumption that the cascade curve fluctuates mainly due to random shifts along axis t .

The formula for correlations between the path of electrons in a layer and a number of electrons at the boundary of the layer follow from the definition $R(t)$ immediately:

$$\text{cov}(N(t), R(t)) = \frac{1}{2} \frac{\partial DR(t)}{\partial t}.$$

The cascades with a fixed point of the first interaction of primary photon

The shift-shaped character of the fluctuations set some authors thinking that it is the influence of fluctuations of the first free path of primary photon. In order to answer this question we used the relationship between two variance: the variance $D(t)$ in EMC with a fixed point of birth of primary photon and the variance $D'(t)$ in EMC with a fixed point of the first interaction of primary photon:

$$\frac{\partial D}{\partial t} + \sigma_\gamma D = \frac{1}{\sigma_\gamma} \left(\frac{\partial \bar{N}}{\partial t} \right)^2 + \sigma_\gamma D'. \quad (40)$$

The calculations EMC in iron from the primary photon with energy 10^3 GeV by threshold energy 0.1 MeV show that the shift-fluctuations are not reduced to primary path fluctuations only. Contributions of the first and the second terms of the right side of the equation (40) into its solution D are comparable in magnitude [94].

The formula (40) will be right and for the path of electrons in layer if we put $\bar{R}(t)$ instead of $\bar{N}(t)$ into the right side of the equation.

The central approach to investigation of random cascade curves

Using the Monte Carlo method Kokoulin and Petrukhin [35] have found that the fluctuations of cascade curve become essentially smaller if to choose $t - \Theta$ as longitudinal variable instead of usual t :

$$N(t) = F_c(t - \Theta),$$

$$\Theta = \int_0^\infty N(t)t dt \left(\int_0^\infty N(t) dt \right)^{-1}.$$

This approach can be named the central approach because the random value Θ is the centre of mass if to regard $N(t)$ as one-dimensional density of mass distribution. Investigation of cascade curve as a whole is the main advantage of this point of view unlike the traditional approach. It gave the possibility to divide the fluctuations of electron number at a fixed depth into shift-fluctuations (because of

random value Θ) and shape–fluctuations as remainder.

The random moment method

In the same time we developed a more general method using the representation

$$N(t) = F_k(t, N^{(0)}, N^{(1)}, \dots, N^{(k)}),$$

$$N^{(i)} = \int_0^\infty N(t) t^i dt. \quad (41)$$

instead of (7). This method was used earlier for mean cascade curve in wellknown works Ivanenko et al. The formula (41) allows to describe the shape of a random curve more detail. In particular it give possibility to decompose the shape fluctuations into large–scale fluctuations, generated by low–order moments, and small–scale ones, generated by high–order moments.

The random moment method is very handy for describing an arbitrary characteristic of cascade curve

$$Q = Q(N(\cdot)) = Q(N^{(0)}, N^{(1)}, \dots, N^{(k)}) \equiv Q(N^{(i)}).$$

If the fluctuations are small enough the mean value and the variance of Q can be written in the following approximation:

$$\langle Q \rangle = Q(\overline{N^{(i)}}) + \frac{1}{2} \sum_{kl} Q_{kl}(\overline{N^{(i)}}) C_{kl},$$

$$DQ = \sum_{kl} Q_k(\overline{N^{(i)}}) Q_l(\overline{N^{(i)}}) C_{kl},$$

where Q_k and Q_{kl} are partial derivatives and C_{kl} obey the equations (26).

The numerical investigation of properties of a set of random moments showed [92,95]:

- fluctuations of $N^{(k)}$ ($k > 0$) have asymptotics like $\delta^2 \sim E^{-1/4}$ though fluctuations of $N^{(0)}$ have another asymptotic $\delta^2 \sim E^{-1}$ as it is told above. ($N^{(0)}$ and R are the same);
- correlations between $N^{(0)}$ and $N^{(k)}$ ($k > 0$) are very weak (they are absent practically for $k > 1$), but ones between $N^{(k)}$ and $N^{(l)}$ ($k > 0, l > 0$) are very intimate, its coefficient equals 1 almost (see the Table 7).

Using this method we investigated such nonadditive characteristics as the center of mass of cascade curve $\Theta = N^{(1)}/N^{(0)}$, the length of cascade $\tau = \sqrt{N^{(2)}/N^{(0)} - \Theta^2}$, the position Θ_m and the value $N(\Theta_m)$ of the maximum of individual (ran-

Table 7
Correlation between longitudinal random moments k_{ij} (air, $E_\gamma = 10^2$ GeV, $E_{th} = 25$ MeV).

k/m	1	2	3	4	5
0	0.178	0.094	0.051	0.021	0.002
1		0.986	0.955	0.908	0.848
2			0.990	0.961	0.915
3				0.990	0.961
4					0.990

dom) cascade curve. The numerical calculation has shown in particular that fluctuations of electron number in individual maximums of cascade are smaller than in the fixed point of maximum of the average cascade and agree with the Poisson's kind. Therefore the first term in (35) can be interpreted as a part of fluctuations which appears due to large-scale fluctuations of random cascade curves.

The lateral moments of electron number

Probabilistic properties of the random lateral distribution is one of the least investigated problem of the cascade theory. Let $\mathbf{r}_1, \dots, \mathbf{r}_v$ be two-dimensional lateral radius–vectors of the electrons crossing a plane which is perpendicular to the direction of primary particle moving. There exist some means to describe such distributions.

The moment method is based on using the random lateral moments

$$\mathbf{r}^{(1)} = \sum_{i=1}^N \mathbf{r}_i, \quad \mathbf{r}^{(2)} = \sum_{i=1}^v r_i^2, \dots \quad (42)$$

The adjoint equations for mean values, variances and covariances of the moments were obtained and solved by our numerical method. The results have shown in particular that the variance of center of mass the random lateral distribution is of the form

$$D \left[\frac{1}{N} \sum_{i=1}^N \mathbf{r}_i \right] \approx \frac{\chi(t)}{N} [1 + \delta_N^2(t)] \overline{r^2},$$

where $\overline{r^2}$ is the mean square lateral spread of the average cascade (see, for example) [96]). The factor χ is a slowly changing function of the depth. Its difference from 1 is inconsistent with the assumption that r_i may be considered as the mutually independent. The numerical values agree with experimental data obtained by measurements of EMC using the counter hodoscope [92]. Besides fluctuations of EMC width and their correlations with N were investigated by the numerical method, too.

Some conclusions from these results were used in the method described below.

Two-component model of space fluctuations

The other way of describing of such distributions is based on the division of the plane into parts ΔS_k and investigation the joint probability for the set of the random numbers $N(\Delta S_1), N(\Delta S_2), \dots, \sum N(\Delta S_i) = N$. As the random moment method gives a smooth random cascade curves it is possible to use the concept of the age s for them. We have supplemented this item by assumption, that the conditional distribution $Prob\{N(\Delta S_1 = n_1), N(\Delta S_2 = n_2), \dots | N = n\}$ is a polynomial distribution. It follows from these assumptions that the square of the relative fluctuations of $N(\Delta S)$ takes the form [97]

$$\delta_{N(\Delta S)}^2 = \delta_{RC}^2 + \delta_{PC}^2. \quad (43)$$

The first term of this sum, so-called regular component, is related to the moment of total particle number by the following way

$$\delta_{PC}^2 = \langle \nu^{2\gamma+2} \rangle / \langle \nu^{\gamma+1} \rangle^2 - 1/\bar{N}, \quad (44)$$

where $\nu = N/\bar{N}$ and γ obeys the equation

$$\langle N(\Delta S, \bar{N})/\bar{N} \rangle = \alpha \nu^\gamma.$$

The second term (Poisson's component) has the usual form

$$\delta_{PC}^2 = \langle N(\Delta s) \rangle^{-1}.$$

The result (44) agrees with fluctuations of all particle number if dimensions of the area ΔS tend to infinity ($\gamma \rightarrow 0$) and with Poisson's fluctuations if the dimensions tend to zero ($\Delta S \rightarrow 0, \gamma \rightarrow \gamma(r)$). This result agrees with Monte Carlo calculations and allows to understand why fluctuations of $N(\Delta S)$ may be less than ones of all particle number N .

It is necessary to note that the second term of the formula (44) must be slightly modified in order to account that Čerenkov's photons come to detector area clustered ones.

Conclusion

The conclusions from above described numerical calculations may be summed in the following way.

Fluctuations of the longitudinal development of EMC are decomposed into shift-fluctuations and shape-fluctuations, and the latter — into large scale and small-scale fluctuations. Small-

scale fluctuations ("rippling") are generated due to random distributions of energy among particles produced in elementary interactions, mainly in bremsstrahlung events. Their value is very sensitive to changing of the threshold energy and depends on the mean particle number as Poisson's fluctuations. Large-scale fluctuations represent random deformations "large-scale" (smooth) cascade curve, connected with fluctuations of central random moments $\int (t - \Theta)^n N(t) dt$. At last shift-fluctuations are connected with fluctuations of center point of the cascade curve $\Theta = N^{(1)}/N^{(0)}$. Shift-fluctuations and the large-scale part of shape fluctuations are generated due to fluctuations of free paths of all particles, mainly photons. These fluctuations are not reduced to effect of the first free path: effects of the first free path and of remaining free paths are comparable. By contrast to "rippling" these fluctuations are produced by high energy part of cascade ($0.01E_0, E_0$) and decreased much slowly with growing of incident energy.

This point of view allows to understand some properties of fluctuations in EMC. The total path of electrons in infinity homogeneous medium is obtained by integrating of cascade curve with respect to co-ordinate t . As a result the contribution of paths disappears and there remain small-scale fluctuations only. Fluctuations of electron paths in thick layers are explained due to effects of cascade curve tails by large-scale fluctuations.

The diversity between different kinds of fluctuations is developed in the maximum of cascade curve. If the particle number is measured in the point of maximum of each random cascade curve we deal with the rippling fluctuations mainly, but if it is measured in the point of maximum of average cascade curve we concern to large-scale fluctuations having the same asymptotic as the first moment ($\delta^2 \sim E^{-1/4}$).

This approach is applicable to spatial fluctuations problem. The first term of sum (43) gives the contribution of fluctuations of spatial distribution due to large-scale fluctuations of cascade curves (because of random values of age). The second (Poisson's) term represents spatial rippling fluctuations which are very sensitive to detector sizes by contrast to the first term.

At last it is necessary to note that these conclusions are made for conventional (BH) showers. The analogous problem is formulated for LPM showers by Misaki. His paper [98] contains the question: "Why is an individual LPM shower so different from the averaged LPM shower?". We think the described above methods will help to find the answer.

8. Sensitivity analysis and generalised importance

Analysis of the sensitivity of various cosmic rays components to the primary spectrum s and medium characteristic variations is an important problem of the theory. Here we consider the role which adjoint formalism plays in the mathematical formulation of several problems of the sensitivity theory.¹

Let $u(x)$ be some known function describing the state of system ‘medium+source+detector’, such as a total cross section, multiplicity, source, medium density, etc. Let $u'(x) = u(x) + \Delta u(x)$, with $\Delta u(x)$ being a variation of u . To study the influence of the variation $\Delta u(x)$ on the detector reading Q , we note that Q is a functional of $u(x)$, that is, Q depends on all the values $u(x)$ taken in the phase space. We therefore denote the detector reading by $J(x, u(\cdot))$. The main goal of the sensitivity theory [9,11] is to find the change in Q , namely

$$\Delta Q(u(\cdot) \rightarrow u'(\cdot)) = Q(u'(\cdot)) - Q(u(\cdot)),$$

due to change of system state u . We may expand ΔQ in a Taylor series

$$\begin{aligned} \Delta Q(u(\cdot) \rightarrow u(\cdot) + \Delta u(\cdot)) &= \\ &= \sum_{n=1}^{\infty} \frac{1}{n!} \int dx_1 \dots \int dx_n \times \\ &\times (Q^{(n)}(x_1, \dots, x_n; u(\cdot)) \Delta u(x_1) \dots \Delta u(x_n)), \end{aligned} \quad (45)$$

where

$$\begin{aligned} Q^{(n)}(x_1, \dots, x_n; u(\cdot)) &= \\ &= \frac{\delta^n Q}{\delta u(x_1) dx_1 \delta u(x_2) dx_2 \dots \delta u(x_n) dx_n} \end{aligned}$$

being the n 'th-order functional derivative. If the functional Q is linear, the equation (45) reduces to

$$\Delta J = \int J^{(1)}(x, u(\cdot)) \Delta u(x) dx \quad (46)$$

which is exact. In accordance with (46) the functional derivative $J^{(1)}(x, u(\cdot)) \equiv \delta J / (\delta u(x) dx)$ gives variation of Q due to unit variation of $u(x)$ in an unit volume about point x . $J^{(1)}$ was called generalised u -importance of point x with respect to functional Q [9,11,100,101]. Such terminology can be justified by the fact that s -importance of point x coincides with usual importance f^+ :

$$J^{(1)}(x, s(\cdot)) = f(x)^+.$$

¹The development of a sensitivity theory based on the use of adjoint functions in the fields of reactor physics and shielding is presented in [13,99].

This expression again demonstrates the important role that the adjoint function, describing here the sensitivity of observable value Q to a point x of primary spectrum s , and hence adjoint formalism plays in the analysis cosmic ray phenomena.

We can also note that d -importance coincides with the particle flux density f ,

$$J^{(1)}(x, d(\cdot)) = f(x),$$

and

$$\begin{aligned} J^{(1)}(x, f^+(\cdot)) &= S(x), \\ J^{(1)}(x, f(\cdot)) &= d(x). \end{aligned}$$

If the functional Q is nonlinear with respect to $u(\cdot)$ the expression (46) holds only at first-order approximation. That is, at first-order approximation the variation of the observable values Q can be presented as

$$\delta Q \approx \int J^{(1)}(x, u(\cdot)) \delta u(x) dx \quad (47)$$

and $J^{(1)}(x, u(\cdot))$ gives (at first-order approximation) variation of Q due to unit variation of $u(x)$. The importance of given equation is that it makes possible to restore a variation $\Delta u(x)$ by solving the inverse problem.

Now let $u(x)$ be a characteristic of the medium only. Functional differentiation (3), (6) with respect to u gives three formulas for u -importance:

$$J^{(1)}(x, u(\cdot)) = \begin{cases} \left(\frac{\delta f^+}{\delta u(x) dx}, s \right), \\ \left(d, \frac{\delta f}{\delta u(x) dx} \right), \\ - \left(f^+, \frac{\delta L}{\delta u(x) dx} f \right). \end{cases}$$

Two of them lead to the necessity of solving equations for functional derivatives

$$\begin{aligned} L^+ \frac{\delta f^+}{\delta u(x) dx} &= - \frac{\delta L^+}{\delta u(x) dx} f^+, \\ L \frac{\delta f}{\delta u(x) dx} &= - \frac{\delta L}{\delta u(x) dx} f. \end{aligned}$$

The third formula is equivalent to the theory of small perturbation [13]

$$\delta Q = \int J^{(1)}(x, u(\cdot)) \delta u(x) dx = -(f^+, \delta L f)$$

and requires the knowledge of two nonperturbate functions f^+ and f .

Both methods are suitable for calculation of u -importance (see, for example [100]). However, in

cosmic ray physics the method based on adjoint function f^+ and equation for functional derivative of adjoint function $\delta f^+ / (\delta u(x) dx)$ is more advantageous since it allows to obtain, at once, all quantities of interest: adjoint function f^+ , detector reading Q , sensitivity function $\delta f^+ / (\delta u(x) dx)$, u -importance $J^{(1)}(x, u(\cdot))$ and variations of the observable value δQ . The calculation scheme is presented in the Fig. 10. Note also that in this case we can use the same numerical method for solving the adjoint equation mentioned above.

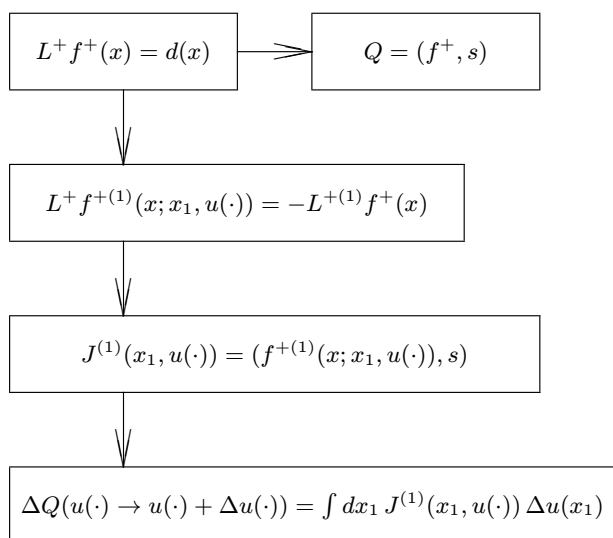


Figure 10. The calculation scheme

9. Sensitivity theory in the problem highest energy EAS simulation

To demonstrate the usefulness and importance of the sensitivity theory in the problem of highest energy EAS simulation, the variations of the EAS characteristics due to the change of the interaction model were investigated [102]. The results obtained within framework of the two different interaction models [103,104] are presented in the Fig. 11, 12, 13. From these figures it is seen that EAS characteristics in model II [104] obtained from EAS data in model I [103] with the help of the eq. (47) do not contradict the results of the direct calculations. In the ovals the contribution of the cross section (σ_p), multiplicity (n_{ch}) and inelasticity coefficient (k) variations on the EAS characteristics are shown also.

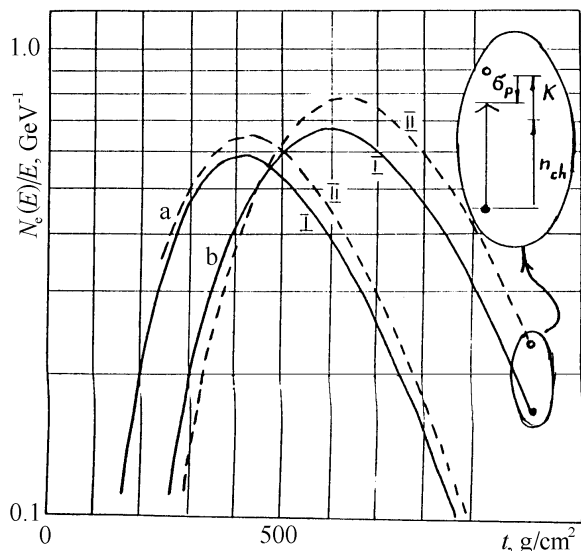


Figure 11. Cascade curves of EAS electrons. a— $E = 10^4$ GeV, b— $E = 10^7$ GeV. I—interaction model [103], II—interaction model [104].

In the oval the contributions of the σ_p , n_{ch} and k variations are shown

10. Sensitivity of cosmic ray muon component to electric field in the atmosphere

To illustrate the general sensitivity theory presented in Sec. 8, here we consider the sensitivity of cosmic ray muon component to electric field in the atmosphere [105].

Alexeyenko et al. [106–108] discussed the nature of the cosmic ray intensity (CRI) microvariations observed for several year with the EAS array of the Baksan neutrino observatory. The microvariations accompanied by thunderstorms and precipitations were found to be produced by substantial perturbations in the atmosphere electric field ². The analysis [108] of the dependence of the variation amplitude of CR muon on the value of electric field has shown that the observed $\sim 1\%$ intensity variations can be explained by a field with a 100–300 MV potential maximum at a 3–4 km altitude. The CRI J_μ was calculated for three profiles of electric field potential (the sinusoidal, exponential and triangular profile) on some assumptions concerning the muon generation function.

Clearly, the approach based on calculating the CRI for a prescribed profile of the field with a subsequent exhaustive search is not optimal for studying the spatial structure of the perturbing field.

²It should be noted that the CRI microvariations were studied earlier [109–111], but explained, however, by the temperature effect

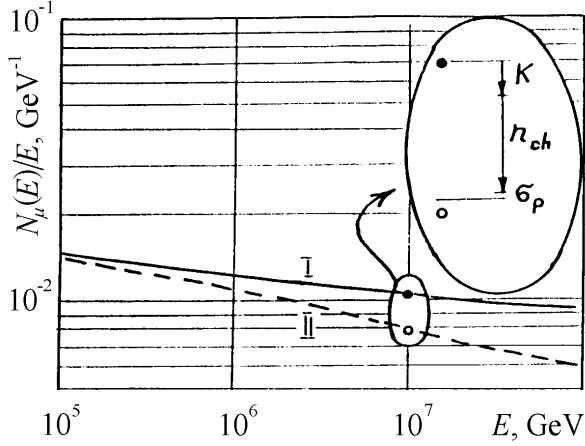


Figure 12. EAS muon number at sea level versus primary proton energy. Muon threshold energy $E_{th} = 1$ GeV. I—interaction model [103], II—interaction model [104].

In the oval the contributions of the σ_p , n_{ch} and k variations are shown

The method which is more convenient uses the coefficients of differential sensitivity of the muon component to the electric field $\alpha_{\mu\pm}^{\mathcal{E}}(z')$,

$$\alpha_{\mu\pm}^{\mathcal{E}}(z') = \frac{1}{J_{\mu}} \frac{\delta J_{\mu\pm}}{\delta \mathcal{E}(z') dz'}, \quad (48)$$

which relates the CRI variations to the electric field intensity perturbations $\delta \mathcal{E}(z')$ as

$$\frac{\delta J_{\mu}}{J_{\mu}} = \int_0^{z^*} dz' (\alpha_{\mu+}^{\mathcal{E}}(z') + \alpha_{\mu-}^{\mathcal{E}}(z')) \delta \mathcal{E}(z'), \quad (49)$$

z^* being observation level. The given method makes it possible in principle to restore the electric field profile by solving the inverse problem [112].

Let the number of muons detected by an array with threshold energy E_{th} be presented as

$$J_{\mu}(z^*, E_{th}) = \sum_{\alpha} \int_{E_{th}}^{\infty} dE s_{\alpha}(E) \times N_{\alpha\mu}(z=0, E|z^*, E_{th}), \quad (50)$$

where s_{α} is the spectrum of primary species α particles, $N_{\alpha\mu} \equiv f_{\alpha}^+$ is the adjoint function of a particle α in this problem, i.e. the contribution of a cascade generated by a single species α particle of energy E at depth z to the measurement value. Since we assume that the cascade develops in the atmosphere in the presence of electric field $\mathcal{E}(z)$ then $N_{\alpha\mu}$ is the field profile functional

$$N_{\alpha\mu} \equiv N_{\alpha\mu}(z, E|z^*, E_{th}; \mathcal{E}(\cdot)),$$

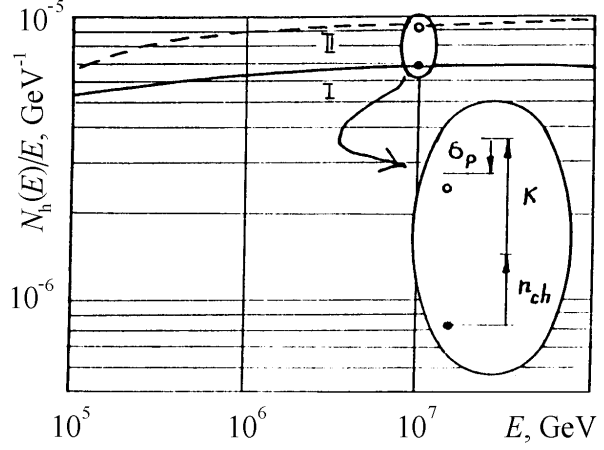


Figure 13. EAS hadron number at mountain level ($t_{obs} = 700$ g/cm²) versus primary proton energy. Hadron threshold energy $E_{th} = 10^3$ GeV. I—interaction model [103], II—interaction model [104].

In the oval the contributions of the σ_p , n_{ch} and k variations are shown

and, therefore,

$$\frac{\delta J_{\mu}}{\delta \mathcal{E}(z') dz'} = \sum_{\alpha} \int_{E_{th}}^{\infty} dE s_{\alpha}(E) \times \frac{\delta N_{\alpha\mu}(z=0, E|z^*, E_{th}; \mathcal{E}(\cdot))}{\delta \mathcal{E}(z') dz'}. \quad (51)$$

From (48) and (50), (51) it is seen that, to calculate the coefficients of differential sensitivity $\alpha_{\mu\pm}^{\mathcal{E}}$ it is sufficient that $N_{\alpha\mu}$ and $\delta N_{\alpha\mu}/(\delta \mathcal{E}(z') dz')$ should be known.

$N_{\alpha\mu}$ is known to satisfy the adjoint equations (6). Assuming that the electric field affects only the muon behavior (the muon mechanism [108]), we may present the above equations and the respective boundary conditions as

$$\begin{aligned} \mathcal{L}^+(p \rightarrow p, n, \pi, K, K^0) N_{p\mu} &= 0, \\ N_{p\mu}(z^*, E) &= 0, \end{aligned} \quad (52)$$

$$\begin{aligned} \mathcal{L}^+(n \rightarrow p, n, \pi, K, K^0) N_{n\mu} &= 0, \\ N_{n\mu}(z^*, E) &= 0, \end{aligned} \quad (53)$$

$$\begin{aligned} \mathcal{L}^+(\pi \rightarrow \pi, K, K^0) N_{\pi\mu} &= 0, \\ N_{\pi\mu}(z^*, E) &= 0 \end{aligned} \quad (54)$$

$$\begin{aligned} \mathcal{L}^+(K \rightarrow \pi, K, K^0) N_{K\mu} &= 0, \\ N_{K\mu}(z^*, E) &= 0, \end{aligned} \quad (55)$$

$$\begin{aligned} \mathcal{L}^+(K^0 \rightarrow \pi)N_{K^0\mu} &= 0, \\ N_{K^0\mu}(z^*, E) &= 0, \end{aligned} \quad (56)$$

$$\begin{aligned} \left[\mathcal{L}^+(\mu \rightarrow \mu) - \frac{\mathcal{E}(z)}{\rho(z)} \cdot 10^{-9} \frac{\partial}{\partial E} \right] N_{\mu\mu} &= 0, \\ N_{\mu\mu}(z^*, E) &= \varepsilon(E - E_{th}), \end{aligned} \quad (57)$$

where

$$\begin{aligned} \mathcal{L}^+(\alpha \rightarrow \{\beta\}) &= -\frac{\partial}{\partial z} + \sigma_\alpha + \sigma_\alpha^r - \\ &- \sum_\beta \int dE' w_{\alpha\beta}(E \rightarrow E') - \sigma_\alpha \int dE' w_{\alpha\mu}(E \rightarrow E'), \end{aligned}$$

σ_α^r is cross section for decay ($\alpha \rightarrow \mu$) of a species α particle; $\rho(x)$ is density of air. The given presentation of the equation for $N_{\mu\mu}$ assumes that the field intensity vector $\vec{\mathcal{E}}(z)$ (\mathcal{E} is measured in V/cm) is directed to the Earth. The superscript (+) corresponds to negative muons μ^- , and the superscript (-) to μ^+ .

By acting on (52-57) from the operator $\delta/(\delta\mathcal{E}(z')dz')$, we obtain the equation for differential sensitivity $\delta N_{\alpha\mu}(z, E)/(\delta\mathcal{E}(z')dz') \equiv N_{\alpha\mu}^\varepsilon(z'; z, E)$. In their form, they coincide with equations (52)-(57),

$$\mathcal{L}^+(\alpha \rightarrow \{\beta\})N_{\alpha\mu}^\varepsilon(z'; z, E) = 0 \quad (58)$$

but have other boundary condition:

$$\begin{aligned} N_{\alpha\mu}^\varepsilon(z'; z', E) &= 0, \quad \alpha = p, n, \pi, K, K^0, \\ N_{\mu\mu}^\varepsilon(z'; z', E) &= \mp 10^{-9} \frac{\partial N_{\alpha\mu}^\varepsilon(z', E)}{\rho(z')\partial E}, \\ N_{\mu\mu}^\varepsilon(z'; z > z', E) &= 0. \end{aligned}$$

Equations (52)-(57) and (58) were solved by the numerical method (see, Sec. 5) for μ^+ and μ^- components separately at zero value of nonperturbed electric field. The inclusive spectra were calculated using the approximations [113] and the model of quark-gluon strings [62]. The calculation were made for the standard atmosphere with the primary proton spectrum $s_p(T) = 16 \cdot T^{1.3}/(10^{-2} \cdot T + 8)^4$ ($[\text{s} \cdot \text{m}^2 \cdot \text{sr} \cdot \text{MeV}]^{-1}$), $T = E_p - mc^2$. The neutron fraction in primary cosmic rays was 17%. Fig.14 presents the coefficients of differential sensitivity $\alpha_\mu^\varepsilon = \alpha_{\mu^+}^\varepsilon + \alpha_{\mu^-}^\varepsilon$ - obtained at threshold energies $E_{th} = 0.2$ and 1.0 GeV ($z^* = 840 \text{ g/cm}^2$).

From Fig.14 it is seen that the coefficients $\alpha_\mu^\varepsilon(z')$ are positive throughout the entire depth interval, i.e. unit variation of electric field intensity in unit

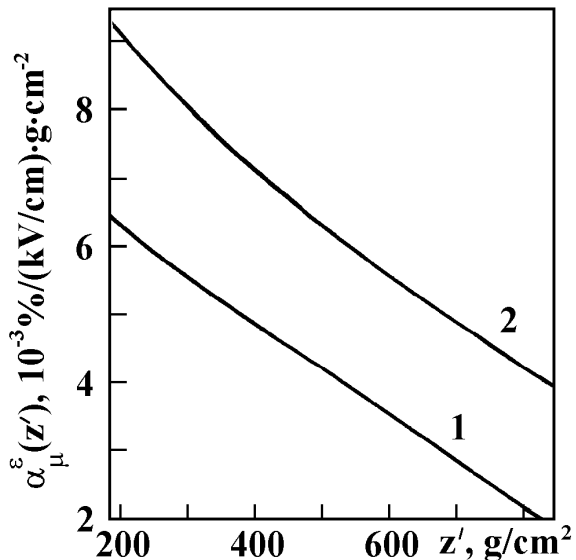


Figure 14. Coefficients of differential sensitivity of muon component to the atmospheric electric field ($z^* = 840 \text{ g} \cdot \text{cm}^{-2}$) at $E_{th} = 0.2$ GeV (1) and 1.0 GeV (2)

layer near z' results in an increased number of detected muons. However an anticorrelation between the value of the field at the observation level and the particle number was observed experimentally [108]. This means that the experimental data can be explained on assumption that the direction of the electric field intensity vector changes at high altitudes.

The muon number variations for the profile of the field

$$\mathcal{E}(z) = \mathcal{E}_0 \rho(z) \cdot \cos \left[\frac{2\pi}{z_0} (840 - z) \right], \quad z \in [360; 840]$$

do not contradict the experimental data [108] for $z_0 = 720 \div 920 \text{ g/cm}^2$ and $\mathcal{E}_0 \approx 10^5 \div 3 \cdot 10^6$ (V/(g·cm⁻²)).

11. The AGN's gamma-ray spectra and their variations in the cascade model

In our papers [114–117] we investigated the variation of the AGNs gamma-ray spectra in the pair-cascade model. According to the cascade model gamma-radiation observed from AGNs results from electron-photon cascade development in X-ray emission region of the source. The electron-photon cascade is caused by pair-production in the photon-X-ray collisions and by inverse Compton

scattering of electrons off X-ray photons. Within the framework of this model one can naturally explain the observed variability of gamma-radiation. Actually, if the formation of an essential part of γ -radiation is due to the cascade development, variability in the X-ray spectra (the medium of cascade development) should induce definite characteristic variations of the gamma-ray spectra (resulting from the cascade development).

We suppose that high-energy electrons ($\alpha = e$) and/or gamma-quanta ($\alpha = \gamma$) with differential energetic spectrum $s_\alpha(E)$ generated in the core propagate through the region of dimension R isotropically filled with X-ray photons with spectral density $n(\omega) = n_0/\omega^\alpha$ in the interval $\omega_1 < \omega < \omega_2$. Allowance is made for e^+e^- -pair production in photon-photon collisions and inverse Compton scattering of electrons off X-ray photons. We are interested in the cascade spectrum of the gamma-quanta escaping the X-ray emission region.

If the dimension of the X-ray emission region R is measured in cascade units $t_0 = (4\pi r_0^2 n_0)^{-1}$, then cascade gamma-ray spectra depend on the value $t = R/t_0$. We now introduce differential energetic spectra $J_\alpha(t, E_{th})$, $\alpha = e, \gamma$, with $J_\alpha(t, E')dE'$ being the mean number of the gamma-quanta with energies between E' and $E' + dE'$, escaping a region of thickness t . $J_\alpha(t, E_{th})$ may be written as

$$J_\alpha(t, E_{th}) = \int s_\alpha(E) q_\alpha(t, E; E_{th}) dE \quad (59)$$

where $q_\alpha(t, E; E_{th}) \equiv q_\alpha(t, E)$ denotes the importance of a primary particle of type α with energy E . For $q_\alpha(t, E)$, the following adjoint cascade equations are valid (see Sec. 1 and [118]):

$$\begin{aligned} & \frac{\partial}{\partial t} q_e(t, E) + \sigma_e(E) q_e(t, E) - \\ & - \int_{E_{th}}^{E_e} dE' w_{e\gamma}(E \rightarrow E') q_\gamma(t, E') - \\ & - \int_{\max\{E_{th}, E-E_e\}}^E dE' w_{e\gamma}(E \rightarrow E-E') q_e(t, E') = 0, \end{aligned} \quad (60)$$

$$\begin{aligned} & \frac{\partial}{\partial t} q_\gamma(t, E) + \sigma_\gamma(E) q_\gamma(t, E) - \\ & - 2 \int_{\max\{E_{th}, E_{\gamma 1}\}}^{E_{\gamma 2}} dE' w_{\gamma e}(E \rightarrow E') q_e(t, E') = \\ & = \delta(t) \delta(E - E_{th}). \end{aligned} \quad (61)$$

Here $w_{e\gamma}$ and $w_{\gamma e}$ are the differential cross-sections of the inverse Compton scattering and pair production, σ_e and σ_γ —the corresponding total absorption cross-sections

$$\begin{aligned} \sigma_e &= \int_0^{E_e} w_{e\gamma}(E \rightarrow E') dE', \\ \sigma_\gamma &= \int_{E_{\gamma 1}}^{E_{\gamma 2}} w_{\gamma e}(E \rightarrow E') dE', \\ E_e &= \frac{E}{1 + E_{ph}/4E}, \\ E_{\gamma 1,2} &= \left(1 \pm \sqrt{1 - E_{ph}/E} \right) \end{aligned}$$

and $E_{ph} = m^2 c^4 / \omega_2$ is the energy threshold of pair production in a given photon field.

The cross sections $w_{\alpha\beta}$ are obtained by integrating the cross sections $w_{\alpha\beta}(E \rightarrow E'; \omega)$ of the interactions in the unit density field of monoenergetic photons with energy ω [119,120] over the X-ray photon spectral density $n(\omega)$

$$\begin{aligned} w_{\alpha\beta}(E \rightarrow E') &= \\ &= \int w_{\alpha\beta}(E \rightarrow E'; \omega) n(\omega) d\omega. \end{aligned} \quad (62)$$

It follows from formulae (59)-(62) that $J_\alpha(t, E_{th})$ is a functional of the functions $n(\omega)$ and $s_\alpha(E)$, so variations of the X-ray photon spectrum as well as variations of the primary cascade-initiating particle spectrum cause changes in the spectrum of escaping gamma-quanta $J_\alpha(t, E_{th})$.

To obtain the functional variations, we use the sensitivity technique presented in Sec. 8. First, one finds the mean value of the functional with realistic values of functions. Next, the sensitivity coefficients are calculated. They represent differential rates of change of the functional with respect to the differential changes in the functions used to calculate the mean value of the functional.

Thus, the functional derivative $\delta J_\alpha(t, E_{th}) / (\delta s_\alpha(E) dE)$ gives the change of $J_\alpha(t, E_{th})$ corresponding to the change per unit of primary particle number inside unit energy range in the vicinity of the point E . Similarly, the functional derivative $\delta J_\alpha(t, E_{th}) / (\delta n(\omega) d\omega)$ gives (in linear approximation) the variation δJ_α as a result of a unit change of $n(\omega)$ in unit energy interval near the point ω . Then the variation δJ_α caused by certain variations $\delta n(\omega)$ and δs_α is written as (taking into account equation (59))

$$\begin{aligned} \delta J_\alpha(t, E_{th}) = & \int dE q_\alpha(t, E) \delta s_\alpha(E) + \\ & + \int dE s_\alpha(E) \int \frac{\delta q_\alpha(t, E)}{\delta n(\omega) d\omega} \delta n(\omega) d\omega. \end{aligned}$$

Thus, it is sufficient to know the importances $q_\alpha(t, E)$ and sensitivity coefficients $\delta q_\alpha(t, E)/(\delta n(\omega) d\omega)$ to calculate the mean gamma-quanta spectra and their variations in the cascade model.

The equations for the sensitivity coefficients $\delta q_\alpha/(\delta n(\omega) d\omega) \equiv q_\alpha^n(t, E)$ may be derived from equations (60), (61) by applying the functional derivative $\delta/(\delta n(\omega) d\omega)$ to the left-hand and right-hand sides of the equations:

$$\begin{aligned} & \frac{\partial}{\partial t} q_e^n(t, E) + \sigma_e(E) q_e^n(t, E) - \\ & - \int_{E_{th}}^{E_e(\omega_2)} dE' w_{e\gamma}(E \rightarrow E') q_\gamma^n(t, E') - \\ & - \int_{\max\{E_{th}, E-E_e(\omega_2)\}}^E dE' w_{e\gamma}(E \rightarrow E-E') q_e^n(t, E') = \\ & = \frac{1}{n_0} \left[-\sigma_e(E; \omega) q_e(t, E) + \right. \\ & + \int_{E_{th}}^{E_e(\omega)} dE' w_{e\gamma}(E \rightarrow E'; \omega) q_\gamma(t, E') + \\ & + \int_{\max\{E_{th}, E-E_e(\omega)\}}^E dE' \times \\ & \left. \times w_{e\gamma}(E \rightarrow E-E'; \omega) q_e(t, E') \right], \quad (63) \end{aligned}$$

$$\begin{aligned} & \frac{\partial}{\partial t} q_\gamma^n(t, E) + \sigma_\gamma(E) q_\gamma^n(t, E) - \\ & - 2 \int_{\max\{E_{th}, E_{\gamma 1}(\omega_1)\}}^{E_{\gamma 2}(\omega_2)} dE' w_{\gamma e}(E \rightarrow E-E') q_e^n(t, E') = \\ & = \frac{1}{n_0} \left[-\sigma_\gamma(E; \omega) q_\gamma(t, E) + 2 \int_{\max\{E_{th}, E_{\gamma 1}(\omega)\}}^{E_{\gamma 2}(\omega)} dE' \times \right. \\ & \left. \times w_{\gamma e}(E \rightarrow E'; \omega) q_e(t, E') \right]. \quad (64) \end{aligned}$$

These differ from equations (60), (61) on their right-hand sides. The equations are then solved numerically. By making test calculations, it has been found that computations of relative variations of the importance $\delta q_\alpha/q_\alpha$ are accurate within a few percent [115].

The mean X-ray spectra from AGNs are accurately described by a single power law with photon spectral indexes α_x around a ‘universal’ value 1.7 [121]. We suppose that the primary cascade-initiating particle spectra are power-laws with indexes ~ 2 , as predicted by shock acceleration models. For given X-ray spectrum the calculated cascade gamma-ray spectrum depends on values of index and cutoffs of the high-energy particles spectrum, and the value of the depth t (in units t_0) as well [118]. These parameters were determined by comparison of the calculated spectra with the observed ones. Using the known expression for the X-ray photon density [122]

$$n(\omega) = \frac{F_x(\omega) d^2}{R^2 c}$$

we obtain

$$t = R/t_0 = 4\pi r_0^2 \frac{F_x(\omega) d^2}{Rc} \omega^{\alpha_x}. \quad (65)$$

Here d is the distance to the source, R – the dimension of the X-ray emission region of the AGN and $F_x(\omega)$ – the observed flux of the X-rays with energy ω . The values of d and F_x are assumed to be known; thus, the value of R can be derived.

NGC 4151.

Fig.15 shows spectrum of the Seyfert galaxy NGC 4151. The mean X-ray spectrum of this galaxy is represented by a single power law spectrum of index $\alpha_x = 1.6$ over the energy range $1 \div 150$ keV. We assumed that electrons with energies $50 \div 10^6$ MeV are generated in the source, and the spectrum is also represented by a single power law of an index $\alpha_e = 2.2$. The calculated mean gamma-ray spectrum (solid curve) well describes the experimental data at the cascade-development region dimension $R = 1.2 \cdot 10^{14}$ cm. This value is obtained provided $d = 20$ Mpc and the 10 keV X-ray photons flux is $F_x = 8 \cdot 10^4$ (cm²·s·keV)⁻¹.

The X-ray variability of the NGC 4151 is now a well-established fact. The soft X-ray photon flux (2 ÷ 10 keV) variations by a factor of 2 ÷ 10 on various time scales ranging from 10 minutes to a few months have been measured. The hard X-ray photon flux variability by a factor of 4 on the time scale of several months can be assumed from observations. Low-energy gamma-ray emission up to

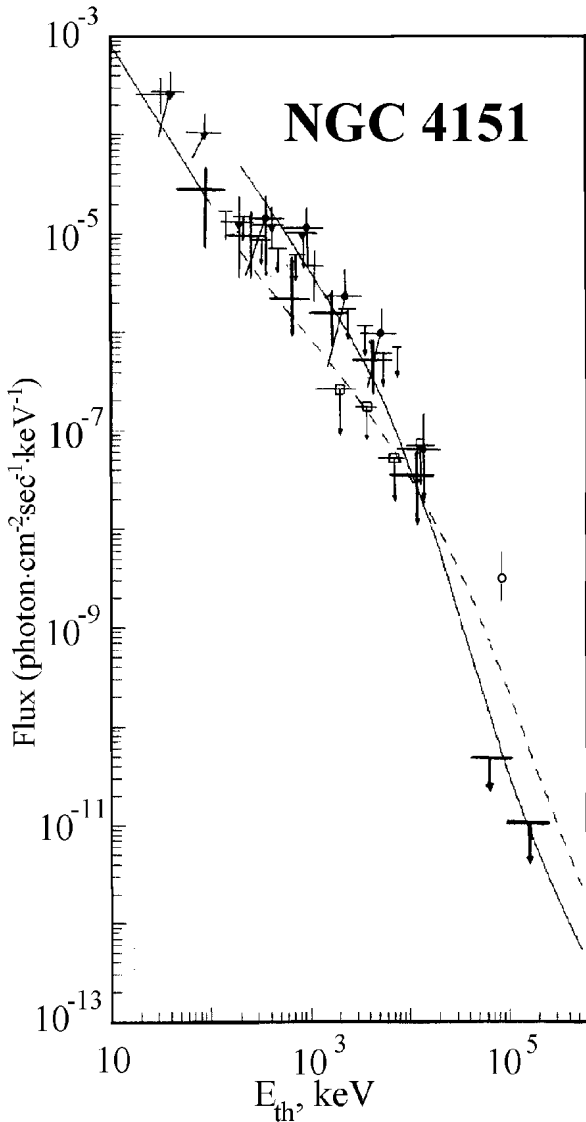


Figure 15. The spectrum of Seyfert galaxy NGC 4151: \circ — [123], the other data from [124]

few MeV shows evidence for intensity variability by a factor of 4 on the same time scale [125]. Over the set of Ginga observations, the $2 \div 10$ keV flux from the source varied by a factor of 4 [126].

We have considered as disturbed the state of the X-ray photon field in which the photon density decreased to one fourth of the mean density (without changing in R). Corresponding gamma-ray spectrum is shown on Fig.15 (dashed curve).

One can see that there exists a characteristic anticorrelation between variations of the gamma-quanta flux with energies below and above 10 MeV: as X-ray luminosity decreases the soft gamma-quanta flux also decreases, while the hard one increases. The calculated variations are the most (by a factor of 7) in the energy range up to 1 MeV and around 100 MeV. The observational data are the

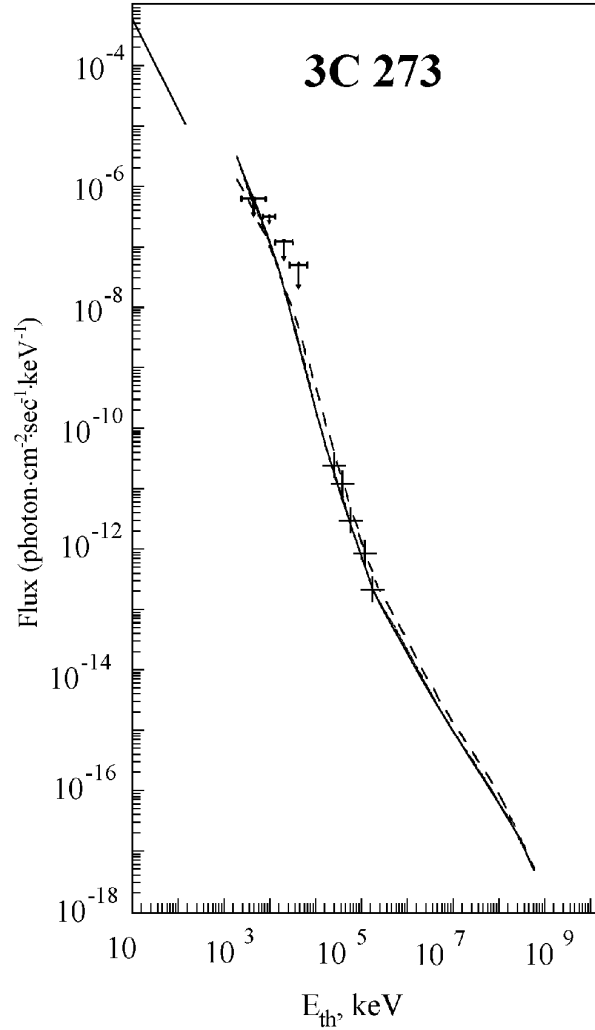


Figure 16. The spectrum of quasar 3C 273. Observational data

\downarrow — [127], \times — [128], \uparrow — [129]

most dispersed in the same regions by a factor of up to 10. Providing that the X-ray flux is varied by a factor greater than 4 (see above) we can well obtain the gamma-ray flux variations by a factor of 10.

If a simultaneous reduction of the cascade-initiating electron spectrum is assumed, the variations in the $0.5 \div 5$ MeV region should increase, while they decrease at ~ 100 MeV due to the above noted anticorrelation. However before making any inferences about the primary electron spectrum change one should take account of softening the X-ray spectrum as the source brightens [124], and possible variations of plasma in the cascade-development region. These factors should give rise to an increase of the gamma-ray spectra variations: the former at high energies, the latter mainly in the vicinity of 0.5 MeV.

3C 273.

Spectrum of quasar 3C 273 is shown in Fig.16. The mean gamma-ray spectrum (solid curve) corresponds to a single power law X-ray spectrum of an index $\alpha_x = 1.7$ in the range $1 \div 150$ keV, with $F_x(10 \text{ keV}) = 6 \cdot 10^4 (\text{cm}^2 \cdot \text{s} \cdot \text{keV})^{-1}$ and $d = 860$ Mpc. Gamma-quanta with energies $10^2 \div 10^6$ MeV are proposed to be generated in the source, $\alpha_\gamma = 2$. The cascade-development region dimension was found to be $R = 1.05 \cdot 10^{17}$ cm.

This quasar is variable in the X-ray band, and variations of the soft X-rays and hard X-rays do not correlate [130,131]. Short time variations at hard X-ray of 41 days has been observed by SIGMA [132]. This is in agreement with our assumption of existence in the object of compact region of hard X-rays emission having a dimension $R \leq 10^{17}$ cm.

Twice, in 1976 and 1978, quasar 3C 273 was observed in hard X-ray and gamma-ray regions nearly simultaneously [128,129]. In the twenty days before the gamma-ray observations in 1976, the X-ray flux may have changed by 40% [131]. According to our

calculations, it should result in the gamma-ray flux changing by 2 (see dashed curve on Fig.16). No variations of the gamma-ray flux between the two observations in 1976 and 1978 was observed within the $\sim 50\%$ uncertainty, but B.N. Swanenburg (in private communication) has noted that flux did change by a factor of 2.

Thus, the gamma-ray spectra of Seyfert galaxy NGC 4151 and quasar 3C 273 and their variations obtained in the cascade model do not contradict the experimental data. To make final conclusions and detail the model one nevertheless need simultaneous observations in the X-ray and the gamma-ray emission regions of the sources.

Acknowledgments

The results presented in this paper reflect a collaborative effort lasting many years. Particularly, we would thank our colleagues G.V. Chernyev, A.I. Goncharov, V.I. Litvinov, A.V. Plyasheshnikov, A.G. Prokopets, S.V. Triphonova, V.V. Vetoshkin for many fruitful discussions.

References

1. Belenky S.Z. Cascade process in cosmic rays (in Russian). Moscow, Gostechizdat, 1948.
2. Rossi B. High energy particles. NJ., Englewood Cliffs, 1952.
3. Nishimura J. Bd. Berlin, 1967, XLVI/2, p.3.
4. Ivanenko I.P. Electromagnetic cascade processes (in Russian). Moscow State University, 1972.
5. Kolchuzhkin A.M., Uchaikin V.V. Introduction in the theory of the particle transport through the matter (in Russian). Moscow, Atomizdat, 1978.
6. Dyakonov M.N., Egorov T.E., Egorova V.P. et al. // Proc. 17 ICRC, Paris, 1981, v.6, p.106.
7. Zatsepin G.T., Sarycheva L.I. // DAN SSSR, 1954, v.99, p.951.
8. Zatsepin G.T., Rozental I.L. // DAN SSSR, 1954, v.99, p.369.
9. Uchaikin V.V., Ryzhov V.V. The stochastic theory of high energy particles transport (in Russian). Novosibirsk, 1988.
10. Uchaikin V.V., Lagutin A.A. Stochastic importance (in Russian). Moscow, Energoatomizdat, 1993.
11. Lagutin A.A., Litvinov V.A., Uchaikin V.V. Sensitivity theory in cosmic ray physics (in Russian). Barnaul, Altai State University, 1995.
12. Lewins J. Importance; the adjoint function. Oxford, 1965.
13. Marchuk G.I., Orlov V.V. // In: Neutron Physics. Moscow, Gosatomizdat, 1961, p.32.
14. Lagutin A.A., Pljasheshnikov A.V., Uchaikin V.V. // Proc. 16 ICRC, Kyoto, 1979, v.7, p.18.
15. Ramakrishnan A. // Proc. Cambridge Phil. Soc., 1950, v.46, p.596.
16. Bhabha H.J. // Proc. Roy. Soc., ser. A, 1950, v.202, p.301.
17. Bhabha H.J., Ramakrishnan A. // Proc. Indian Acad. Sci., ser. A, 1950, v.32, p.141.
18. Janossy L. // Proc. Phys. Soc., ser. A, 1950, v.63, p.241.
19. Bharucha-Reid A.T. Elements of the theory of Markov processes and their applications. MC Grow-Hill Book Company, NY-Toronto-London, 1960.

20. Ramakrishnan A. Elementary particles and cosmic rays. Pergamon Press, Oxford–London–NY–Paris, 1962.
21. Gerasimova N.M. // Trudi FIAN SSSR, 1964, v.26, p.191.
22. Gedalin E.V. // In: Physics of high energy particles, Tbilisi, 1966, v.2, p.5.
23. Lengeler E., Tejessy W., Deutschmann M. // Zeitschrift für Physik, 1963, v.175, p.283.
24. Emeljanov Yu.A. // Proc. 15th ICRC, Plovdiv, 1977, v.7, p.472.
25. Gladki A., Jablonski Z. // Acta Universitatis Lodziensis, ser. 2, 1977, v.12, p.99.
26. Srinivasan S.K. et al. // Zeitschrift für Physik, 1961, v.161, p.346; 1964, v.177, p.164.
27. Uchaikin V.V., Lagutin A.A. // Proc. 15th ICRC, Plovdiv, 1977, v.7, p.490.
28. Kalmykov N.N., Chistjakov V.P. // Izvestia AN SSSR, ser. fiz., 1965, v.29, p.1702.
29. Uchaikin V.V., Pljasheshnikov A.V., Lagutin A.A. et al. // Proc. 15 ICRC, Plovdiv, 1977, v.7, p.502.
30. Uchaikin V.V., Plyasheshnikov A.V., Lagutin A.A. et al. // Izvestia vuzov SSSR, Fizika, 1978, N 4, p.27.
31. Pljasheshnikov A.V., Lagutin A.A., Uchaikin V.V. // Proc. 16 ICRC, Kyoto, 1979, v.7, p.1.
32. Pljasheshnikov A.V., Lagutin A.A., Uchaikin V.V. // Proc. 16 ICRC, Kyoto, 1979, v.7, p.13.
33. Lagutin A.A., Uchaikin V.V., Chernyaev G.V. // Proc. 17 ICRC, Paris, 1981, v.6, p.260.
34. Uchaikin V.V. // Izvestia vuzov SSSR, Fizika, 1978, N 12, p.30; 1979, N 2, p.7; 1979, N 8, p.14.
35. Kokoulin R.P., Petrukhin A.A. // Journal of Nuclear Physics (USSR), 1980, v.32, p.1030.
36. Vetoshkin V.V., Lagutin A.A., Chernyaev G.V. Preprint ASU-92/2, Barnaul, 1992, 19 p.
37. Lagutin A.A., Pljasheshnikov A.V., Uchaikin V.V. et al. // Proc. 17 ICRC, Paris, 1981, v.5, p.202.
38. Lagutin A.A., Pljasheshnikov A.V., Uchaikin V.V. // Proc. 17 ICRC, Paris, 1981, v.5, p.194.
39. Lagutin A.A., Uchaikin V.V., Chernyaev G.V. et al. Preprint LNPI N1289, Leningrad, 1987, 60 p.
40. Goncharov A.I., Konopelko A.K., Lagutin A.A. et al. // Izv. AN SSSR. Ser. fiz., 1991, v.55, p.724.
41. Goncharov A.I. Ph. D. Thesis, Altai State University, 1991, 145 p.
42. Nagel H.H. // Z. Physik, 1965, Bd 186, p.319.
43. Belousov A.S., Malinovsky E.I., Rusakov S.V. et al. // Yad. Fiz., 1973, v.17, p.1028.
44. Borkovsky M.J., Kruglov S.P. // Atomnaya Energiya, 1976, v.40, p.243.
45. Adler D., Fuchs B., Thielheim K.O. // Proc. 15 ICRC, Plovdiv, 1977, v.7, p.466; 1977, v.20, N6, p.513.
46. Belyaev A.A., Guzhavin V.V., Ivanenko I.P. Preprint FIAN N34, Moscow, 1975, 37 p.
47. Varfolomeev A.A., Drabkin L.B. // In: Cosmic Rays, N12. Moscow, 1970, p.32.
48. Konishi E., Misaki A., Fujimaki N. CRL Report 36-76-3, 1976; Nuovo Cim., 1978, v.44a, N 4, p.509.
49. Ellsworth R.W., Streitmatter R.E., Bowen T. // Proc. 16 ICRC, Kyoto, 1979, v.7, p.55.
50. Kolchuzhkin A.M., Bepalov V.I. // Proc. 16 ICRC, Kyoto, 1979, v.9, p.222.
51. Hillas A.M., Lapikens J. // Proc. 15 ICRC, Plovdiv, 1977, v.8, p.460.
52. Hillas A.M. // J. Phys. G.: Nucl. Phys., 1982, v.8, p.1461.
53. Plyasheshnikov A.V., Vorobjev K.V. // Proc. 17 ICRC, Paris, 1981, v.5, p.206.
54. Kolchuzhkin A.M., Uchaikin V.V., Bepalov V.I. // Izv. AN SSSR. Ser. fiz., 1973, v.7, p.1442.
55. Muller D. // Phys. Rev. D., 1972, v.5, p.2677.
56. Barmin V.V., Varylov V.G., Golubchikov V.M. et al. Preprint ITEP, Moscow, 1972, 12 p.
57. Hillas A.M. // Proc. 17 ICRC, Paris, 1981, v.6, p.244.
58. Vorobjev K.V., Plyasheshnikov A.V., Uchaikin V.V. // Izv. AN SSSR. Ser. fiz., 1982, v.46, p.2437.
59. Plyasheshnikov A.V., Konopelko A.K., Vorobjev K.V. Preprint FIAN N92, Moscow, 1988, 48 p.
60. Lagutin A.A., Plyasheshnikov A.V., Melentyeva V.V. Preprint of the Altai State University (Barnaul), N 96/2, 1996.
61. Lagutin A.A., Plyasheshnikov A.V., Goncharov A.I. // Nucl. Phys. B (Proc. Suppl.), 1998, v.60B, p.161.
62. Shabelski Yu.M. // Yad. Fiz., 1986, v.44, p.186; v.45, p.223.

63. Chernyaev G.V. Ph. D. Thesis, Altai State University, 1987, 173 p.
64. Dyakonov M.N. et al. // In: Cosmic rays with energy $E > 10^{17}$ eV (in Russian), Yakutsk, 1983, p.34.
65. Aseikin V.S., Dubovy A.G., Kabanova N.V. et al. // 15 ICRC, Plovdiv, 1977, v.8, p.98.
66. Nagano M., Hatano Y., Hara T. et al. // J. Phys. Soc. Jap., 1984, v.53, p.1667.
67. Khristiansen G.B. et al. // 18 ICRC, Bangalore, 1983, v.9, p. EA 1.1-9.
68. Diminstein O.S. et al. // In: Cosmic rays with energy $E > 10^{17}$ eV (in Russian), Yakutsk, 1983, p.30.
69. Hillas A.M. // Proc. the Cosmic Ray Workshop University of Uta, 1983, p.16.
70. Gaiser T.K., Protheroe R.J., Turver K.E. et al. // Rev. Mod. Phys., v.50, p.859.
71. Antonov R.A., Ivanenko I.P., Samosudov B.E. et al. // Izv. AN SSSR. Ser. fiz., 1971, v.35, p.2113.
72. Antonov R.A., Ivanenko I.P., Tulinova Z.I. // Yad. fiz., 1973, v.18, p.554.
73. Rozental I.L., Streltsov V.N. // J. Exper. Teor. Fiz., 1958, v.35, p.1440.
74. Zatsepin G.T., Mikhanchi E.D. // J. Phys. Soc. Japan, Suppl. A-111, 1962, v.17, p.356.
75. Nishimura J. // Proc. ICRC, Jaipur, 1964, v.6, p.224.
76. Zatsepin G.T., Mikhanchi E.D. // Proc. 9 ICRC, London, 1965, v.2, p.224.
77. Kobayakawa K. // Nuovo Cim., 1967, v.B47, p.156.
78. Gurentsov V.I., Zatsepin G.T., Mikhanchi E.D. // Yad. Fiz., 1976, v.23, p.1001.
79. Gurentsov V.I. Preprint INR, N P-0379, Moscow, 1984; Preprint INR, N P-0380, Moscow, 1984.
80. Bugaev E.V., Naumov V.A., Sinogovskiy S.I. // Izv. AN SSSR. Ser. fiz., 1985, v.49, p.1349.
81. Bilokon H., Castellina A., D'Ettorre Piazzoli B. et al. // NIM, 1991, v.A303, p.381.
82. Lipari P., Stanev T. // Phys. Rev. D., 1991, v.44, p.3543.
83. Lagutin A.A., Prokopets A.G., Konopelko A.K. et al. // Proc. 22 ICRC, Dublin, 1991, v.2, p.752.
84. Lagutin A.A., Prokopets A.G., Uchaikin V.V. // Izv. RAN. Ser. fiz., 1993, v.57, p.145.
85. Besrukov L.B., Bugaev E.V. // Proc. 17 ICRC, Paris, v.7, p.102.
86. Besrukov L.B., Bugaev E.V. // Yad. fiz., 1981, v.33, p.1195.
87. Kokoulin R.P., Petrukhin A.A. // Proc. 11 ICRC, Budapest, 1969, v.4, p.277.
88. Uchaikin V.V., Lagutin A.A., Pljasheshnikov A.V. // Journal of Nuclear Physics (USSR), 1979, v.30, p.429.
89. Lagutin A.A., Pljasheshnikov A.V., Uchaikin V.V. // Proc. 17th ICRC, Paris, 1981, v.5, p.198.
90. Uchaikin V.V., Lagutin A.A. // Izvestia AN SSSR, ser. fiz., 1978, v.42, p.1458.
91. Uchaikin V.V., Lagutin A.A. // Journal of Nuclear Physics (USSR), 1975, v.21, p.1257.
92. Vetoshkin V.V., Uchaikin V.V., Preprint IFVE AN of Kazakh SSR, Alma-Ata, 87/12, 1987.
93. Uchaikin V.V., Lagutin A.A. // Izvestia AN SSSR, ser. fiz., 1976, v.40, p.1068.
94. Vetoshkin V.V., Lagutin A.A., Uchaikin V.V. // Izvestia AN SSSR, ser. fiz., 1980, v.44, p.575.
95. Vetoshkin V.V., Uchaikin V.V. // Izvestia vuzov SSSR, Fizika, 1987, v.3, p.17.
96. Misaki A. // Suppl. Progr. Theor. Phys., 1964, v.32, p.82.
97. Uchaikin V.V., Chernjaev G.V. // Journal of Nuclear Physics (USSR), 1989, v.50, p.736.
98. Misaki A., // Nucl. Phys. B. (Progr. Suppl.), 1993, v.33B, p.192.
99. Usachev L.N. // J. Nucl. Energy, 1964, v.18, p.541; Pomraning G.S. // J. Math. Phys., 1967, v.8, p.149; Oblova E.M. ORNL-TM-4110, Oak Ridge, 1973; Weisbin C.R., Oblova E.M., Marable J.H. et al. // Nucl. Sci. Eng., 1978, v.66, p.307; Cacuci D.G., Weber C.F., Oblova E.M. et al. // Nucl. Sci. Eng., 1980, v.75, p.88.
100. Litvinov V.A. Ph. D. Thesis, Altai State University, 1986, 98 p.
101. Lagutin A.A., Litvinov V.A., Uchaikin V.V. // Proc. 20 ICRC, Moscow, 1987, v.4, p.276.
102. Lagutin A.A., Litvinov V.A., Nikulin Yu.A. et al. // Nuclear Phys. B (Proc. Suppl.), 1997, 52 B, p.158.

103. I. P. Ivanenko, B. L. Kanevsky, T. M. Roganova // *Yad. fiz.*, 1979, v.29, p.694.
104. N. N. Kalmykov, G. B. Khristiansen // *Pis'ma JETP*, 1983, v.37, p.247.
105. Dorman L. I., Lagutin A. A., Chernyaev G. V. // *Proc. 21 ICRC, Adelaide*, 1990, v.7, p.92.
106. Alexeyenko V. V., Sborshikov V. G., Chudakov A. E. // *Izv. AN SSSR. Ser. fiz.*, 1984, v.48, p.2152.
107. Alexeyenko V. V., Chudakov A. E., Sborshikov V. G. et al. // *Proc. 19 ICRC, La Jolla*, 1985, v.5, p.352.
108. Alexeyenko V. V., Chernyaev A. V., Chudakov A. E. et al. // *Proc. 20 ICRC, Moscow*, 1987, v.4, p.272.
109. Fazzini M. C., Galli M., Guidi I. et al. // *Can. J. Phys.*, 1968, v.46, p.1073.
110. Attolini M. R., Cecchini S., Galli M. et al. // *Let. Nuovo cim.*, 1971, v.1, p.716.
111. Attolini M. R., Cecchini S., Galli M. et al. // *Let. Nuovo cim.*, 1971, v.2, p.329.
112. Nikulin Yu. A. // *Proc. 27 VNSK. Ser. Fiz., Novosibirsk*, 1989, p.9.
113. Kalinovsky A. N., Mokhov N. V., Nikitin Yu. P. Passage of high energy particles through matter (in Russian). Moscow, Energoatomizdat, 1985.
114. Ivanenko I. P., Lagutin A. A., Linde I. A. et al. // *Proc. 22 ICRC, Dublin*, 1991, v.1, p.121.
115. Ivanenko I. P., Lagutin A. A., Triphonova S. V. Preprint ASU-92/4, Barnaul, 1992, 53 p.
116. Ivanenko I. P., Lagutin A. A., Triphonova S. V. // *Vestnik MSU. Ser.3. Fiz. Astr.*, 1993, v.34, p.69.
117. Triphonova S., Lagutin A. // In: *Progress in New Cosmologies: Beyond the Big Bang*. Plenum Publ. Corp., NY., 1993, p.259.
118. Ivanenko I. P., Lagutin A. A., Linde A. A. et al. Preprint NPI MSU 91-24/228, Moscow, 1991, 46 p.
119. Aharonian F. A., Kirillov-Ugryumov V. G., Vardanian V. V. // *Astrofizika*, 1984, v.20, p.223.
120. Aharonian F. A., Kirillov-Ugryumov V. G., Vardanian V. V. // *Astrophys. and Space Sci.*, 1985, v.115, p.201.
121. Turner T. J., Weaver K. A., Mushozky R. F. et al. // *Astrophys. J.*, 1991, v.381, p.85.
122. Herterich K. // *Nature*, 1978, v.250, p.311.
123. Halper A. M., Kirillov-Ugryumov V. G., Luchkov B. I. et al. // *Pisma J. Exper. Teor. Fiz.*, 1973, v.17, p.265.
124. Perotti F., Della Ventura A., Villa G. et al. // *Astrophys. J.*, 1981, v.247, p.63.
125. Perotti F., Maggioli P., Quadrini E. et al. // *Astrophys. J.*, 1991, v.3732, p.75.
126. Yagoov T., Warwick R. S. // *Proc. 23 ESLAB Symp. Bologna*, 1989, v.2, p.1089.
127. White R. S., Dayton B., Gibbons R. // *Nature*, 1980, v.284, p.608.
128. Swanenburg B. N., Bennet K., Bignami G. F. et al. // *Nature*, 1978, v.275, p.298.
129. Bignami G. F., Bennet K., Buccheri R. et al. // *Astron. Astrophys.*, 1981, v.93, p.71.
130. Dean A. J., Bazzano A., Court A. J. et al. // *Astrophys. J.*, 1990, v.349, p.41.
131. Courvoisier T. J.-L., Turner M. J. L., Robson E. I. et al. // *Astron. Astrophys.*, 1987, v.176, p.197.
132. Bassini L. et al. // *Astrophys. J.*, 1992, v.396, p.504.